NMR Study on the Aggregation Behavior of the Therapeutic Peptide Carbetocin

DEPARTMENT OF FOOD TECHNOLOGY, ENGINEERING AND NUTRITION | LUND UNIVERSITY
FRIDA TERNE | MASTER THESIS IN PHARMACEUTICAL TECHNOLOGY 2018

LUND
UNIVERSITY

NMR STUDY ON THE AGGREGATION BEHAVIOR OF THE THERAPEUTIC PEPTIDE CARBETOCIN

30hp MSc Thesis in Pharmaceutical Technology

Author: *Frida Terne*

Industrial supervisor: *Dan Lundberg, CR Competence*

Academic supervisor: *Ola Wendt, Centre for Analysis and Synthesis*

Examiner: *Marie Wahlgren, Department of Food Technology*

Lund University

Spring Semester 2018

1 Abstract

Carbetocin is an uncharged cyclic therapeutic peptide with a tendency to aggregate in solution. Aggregation is undesirable since it, for example, can lead to loss of pharmaceutical effects. To gain a better understanding of peptide aggregation, along with a potential to develop better drug formulations, aggregation of carbetocin was studied. In focus were soluble aggregates in contrast to phase-separated aggregates. The behavior of these soluble aggregates was studied with NMR spectroscopy. NMR diffusometry and ^{1}H NMR spectroscopy were used as the main analytic methods. Aqueous solutions of carbetocin at different concentrations alone, and with added sodium dodecyl sulfate (SDS) and pentaethylene glycol monododecyl ether ($C_{12}E_5$) were analyzed using these methods. The peptide has an increased self-aggregation in solution at higher peptide concentrations, with a distinct increase in aggregation at around 15-20 mM carbetocin. Hydrophobic interactions and hydrogen bonding are suggested to be the major attractive forces in the aggregation mechanism based on that the chemical shifts of hydrophobic and hydrogen-bonding sites in carbetocin show significant changes at higher peptide concentrations. Surfactants significantly affect the aggregation behavior of carbetocin and co-aggregates are formed. To fully understand the aggregation behavior of carbetocin and other peptides, more research has to be conducted.

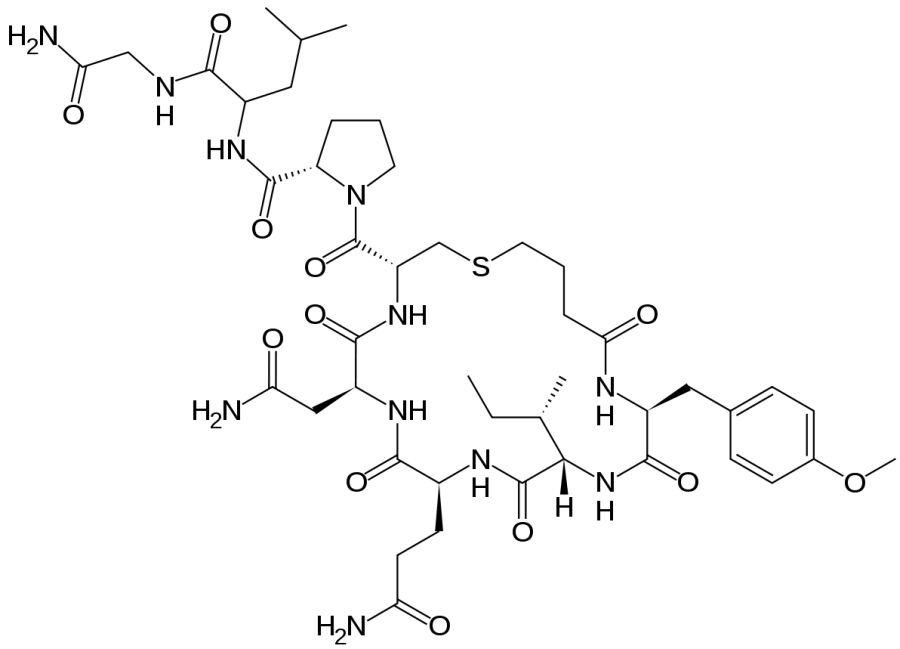

Figure 1: The model peptide used in this work, carbetocin

2 List of abbreviations

$\Delta\delta$	-	Change in chemical shift
API	-	Active pharmaceutical ingredient
$C_{12}E_5$	-	Pentaethylene glycol monododecyl ether
CAC	-	Critical aggregation concentration
Carb	-	Carbetocin
CD	-	Cyclodextrin
CMC	-	Critical micelle concentration
COSY	-	Correlation spectroscopy
δ	-	Chemical shift
D	-	Diffusion coefficient
D_2O	-	Deuterium
DMSO	-	Dimethyl sulfoxide
dNMR	-	Diffusion NMR
HSQC	-	Heteronuclear single-quantum correlation
MBCD	-	Methyl-β-cyclodextrin
NMR	-	Nuclear magnetic resonance
NOE	-	Nuclear Overhauser effect
PPI	-	Peptide-peptide interactions
ppm	-	Parts per million
r_H	-	Hydrodynamic radius
ROESY	-	Rotating-frame nuclear Overhauser effect correlation spectroscopy
SDS	-	Sodium dodecyl sulfate
UV	-	Ultra-violet (light)

Table of contents

3 Introduction

Peptide pharmaceuticals is a multibillion-dollar industry with over hundred new drugs undergoing clinical trials during 2015 [1]. These drugs provide treatment of a wide variety of diseases and conditions with advantages over small organic molecules and proteins. Peptides often provide a greater selectivity and specificity for their drug target and hence often being more efficient. Compared to proteins, peptides are smaller, and can hence penetrate further into target tissues as well as often having a lower cost of production since they can be synthetically produced [2]. Insulin is probably the most well-known peptide drug with its use in treating diabetes, however there are peptide drugs being used as antibiotics and cancer treatments as well [2].

However, compared to small molecule drugs, these larger pharmaceuticals also pose many challenges. Firstly, the clearance of peptides in the body is fast due to the presence of enzymatic proteases and the renal and hepatic clearance is fast. Additionally, the bioavailability is low since peptides generally have a hydrophilic nature and cannot easily cross bodily barriers, and hence a parenteral (injected via a needle into the body at various sites and depths) [3] formulation is usually needed. For parenteral formulations, the drug is often in an aqueous solution, lipid formulations and oil-based suspensions exist as well, and there is a limit of how much liquid can be injected to a human. One of the major challenges with peptide pharmaceuticals is their instability in solution. Unstable peptides formulations may lose their pharmaceutical effect and/or become immunogenic (causing an immune response). Additionally, aggregated solutions can clog syringes and make administration hard. The instability can be of chemical nature as in molecular degradation, when new chemical entities are formed by covalent bonds are being formed or cleaved [4]. The stability issue can also be physical, which is changes in the structural features of the molecule(s). Aggregation is such a physical change [5] and the focus in this master thesis work.

Aggregation of peptides is affected by numerous aspects. High peptide concentration, high temperature, and mechanical stress [6] are just three factors which generally increase peptide aggregation [5]. The temperature dependence, where higher temperatures often increases aggregation, can pose a problem for transport and storage. Concerning transport, there are cold containers for transport, but their use is more complicated and expensive. For storage, in hospitals in Sweden and other parts of the world where the health care system is well developed, cold storage is a standard. However, for countries in a warmer climate and with less developed health care, this could be hard to solve [7]. Special demands for storage can also pose a problem for patients using the drug daily or several times a day. The mechanical stress dependence may also pose a problem during transport and storage, mainly the risk of shaking. During road transport, shaking is inevitable and if the drug is used by patients in their everyday lives, it might be exposed to shaking e.g. from being carried in a bag. Concerning the concentration dependence, for high potency drugs one may be able to go down in concentration and up in injected volume, however, for low potency drugs, this is not an option since the injected fluid volume would be too large. Carbetocin (the model peptide used in this thesis work) is currently used in low concentration, 0.1 mg/ml. However, research has been conducted on using carbetocin for other indications, which would require a higher concentration and hence, problems could occur [8].

Although an important topic, research about peptide aggregation is lacking according to literature search during this project as well as claimed in published work [5]. Additionally, general knowledge

about the physical chemistry of therapeutic peptides might be lacking. Since an understanding of the physical chemistry of the active pharmaceutical ingredient (API) is not needed to get a drug approved, if all pharmaceutical effects are well-known and thoroughly explained, research about the physical chemistry is not prioritized in all cases. Hence, apart from the pharmaceutical applications of studying peptide aggregation to design better formulations, a deeper fundamental knowledge about peptides' physical chemistry and how it is affected by co-solutes is of interest. Peptide physical instability and specifically peptide aggregation has been the focus of this work.

NMR spectroscopy is widely used in chemistry and pharmaceutical industry for e.g. characterization, structure determination and study of physical aspects of chemical systems. Using diffusion NMR spectroscopy (dNMR), the self-diffusion coefficient of molecules/aggregates can be obtained and hence an idea about a molecule's/aggregate's effective size is achieved. However, apart from using dNMR to study the presence of different sized molecules/aggregates in a solution [9][10], NMR spectroscopy has not extensively been used to study aggregation of peptides. NMR spectroscopy was selected as the major analytical method used in this master thesis work.

4 Aim

The aim of this project is to investigate the aggregation behavior of the therapeutic peptide carbetocin. Peptide aggregation is a problem within the pharmaceutical industry and hence a better understanding of the phenomenon is of big interest. To study aggregation the small, therapeutic peptide carbetocin was selected as a model. Different forms of aggregates exist, generally divided, there are phase-separated or precipitated aggregates and soluble aggregates or self-assembly in solution. The main focus of this work is to study the soluble aggregates. Peptide-peptide interactions are important in understanding peptide aggregation, soluble as well as phase-separated, and the forces involved in carbetocin's self-aggregation were studied by trying to understand which parts of the molecule have a major role in the aggregation. Additives may alter the aggregation behavior of peptide and therefore certain additives, mainly surfactants, were studied in order to further understand the self-aggregation of the peptide as well as the possible formed co-aggregates. Even though the soluble aggregates are the focus in this work, an understanding of how these soluble aggregates are related to the phase-separated aggregates is also of interest. To study the above, NMR spectroscopy was selected as the main method. ^{1}H NMR and dNMR are the two major NMR spectroscopy techniques applied.

5 Theoretical and experimental background

5.1 Forces in peptide aggregation

In order for peptides to aggregate, peptide-peptide interactions (PPIs) of attractive nature have to be present. For charged peptides the charge-charge, charge-dipole or charge-induced dipole interactions are long to medium range, meaning that the molecules affect each other even at longer distances and hence affecting the PPIs to a large extent. The charge-charge interaction is often repulsive (reducing aggregation), since peptides and proteins most often hold a negative charge, whereas the other two are attractive and hence inducing aggregation. For uncharged peptides as carbetocin, the model peptide in this work, other forces are present. These are forces such as hydrophobic interaction, van der Waal's interactions, hydrogen bonding and aromatic stacking. These can all be attractive forces and are only short ranged [5] and hence not affecting the peptides as much as charge-interactions. However, if no long-range forces are present, the short-ranged forces become significant. Van der Waals interactions are dipole-dipole, dipole-induced-dipole and induced dipole-induced dipole interactions that are due to fluctuations in the electron density in the atoms. Hydrogen bonding is the interaction between an electron-deficient hydrogen atom attached to an electronegative atom such as oxygen or nitrogen and an electron-rich atom such as oxygen or nitrogen, these dipoles of different character are strongly attracted to each other [11]. Aromatic stacking is the attractive force between two aromatic systems. An electron rich part of one aromatic ring interacts with an electron deficient part of another aromatic ring. The hydrophobic interactions are due to that the hydrophobic parts of a molecule try to have minimal contact with the surrounding water, and hence hydrophobic parts are attracted to each other to exclude the surrounding water [11]. Depending on the peptide, different forces are dominant.

5.2 Peptide aggregation

Peptides are similarly to proteins made up of an amino acid backbone, although peptides have fewer amino acid residues than proteins. Several definitions of peptides exist, usually they are defined as an amino acid sequence of up to 50 residues which lack the higher ordered structure of proteins [5].

The stability of proteins and peptides is of importance in many applications and especially when used in pharmaceuticals, since physical instability of the drug formulation and chemical instability of the API can lead to loss of desired function and/or cause immunogenic effects [5]. Chemical degradation includes, but is not limited to, de-amidation, oxidation and hydrolysis [12], however the focus of this report is physical stability. There are several ways in which loss of physical stability can occur, such as denaturation, surface adsorption and aggregation [12]. Denaturation is more of concern for proteins which have a higher-ordered structure and not for peptides. The 3D structure of proteins is typically critical for their pharmaceutical effect and since it is often lacking for smaller peptides this is not a major problem. However, aggregation and surface adsorption can happen to peptides as well as proteins. Surface adsorption of peptides can be problematic and has been studied elsewhere [13][14]. Aggregation is the form of physical instability studied in this work. Due to the difference in conformational structure between proteins and peptides, they usually have different mechanisms of aggregation. In peptides, it is believed that hydrophobic side chains usually are the driving force to aggregation [15]. In proteins, the same forces are present, however, the hydrophobic side chains are usually buried within the protein, excluded from the surrounding water and hence a (partial) denaturation is often the driving force for aggregation for proteins.

The physical stability of peptides is affected by numerous things, e.g. pH and ionic strength, addition of additives [16], peptide concentration [17] and temperature. Depending on the peptide, the physical stability is affected differently. How an increase in peptide concentration increases soluble aggregation is intuitive since there are more molecules in the solvent and the risk of interaction is higher and hence being a general aggregation-inducing aspect. However, it is not clear that an increase in concentration will increase phase-separated or precipitated aggregation, it could potentially be that soluble aggregates stabilize a solution from phase-separating in a way similar to how micellar solutions under the Krafft point, the temperature which sets the onset of markedly increasing the solubility of surfactants [18], could be more stable than monomeric solutions. Addition of other components to the aqueous peptide solution may affect the aggregation in various ways depending on the additive and the peptide properties. A common way to control peptide aggregation is pH adjustment of the solvent to induce charges on the peptide and hence induce repulsive forces which reduce aggregation [6]. However, there are uncharged pharmaceutical peptides, e.g. carbetocin, for which this approach cannot be utilized.

The most discussed and investigated way of peptide/protein aggregation is amyloid formation, which is generic for all peptides/proteins since it is based on the interactions between the backbones of peptides [19]. These fibrillary, amyloid structures are probably most well known for their relation to certain neurodegenerative diseases including Alzheimer's disease and Parkinson's [20]. Since the discovery of this relation, a lot of research has been conducted upon amyloid formation, but how and why these protein fibrils are formed is not yet fully understood. Although amyloid formation is generic for all peptides/proteins, other forms of aggregation exist. Høgstedt et al's showed that carbetocin form non-structured precipitated aggregates [6].

Aggregates are for many equivalent to these amyloid precipitates. However, peptides can in addition to amyloid fibrils form soluble non-structured aggregates, and the mechanism for soluble peptide aggregation and its relation to phase-separated aggregates and/or amyloid fibrils has not been extensively studied. One hypothesis of this project is that non-structured soluble aggregates may form prior to the phase-separated aggregates whether they be amyloids or not. However, there is limited research on soluble peptides and hence it is hard to say whether or not this hypothesis is adopted by the scientists in the field. It is these soluble aggregates that are the focus of this report.

1.1 Carbetocin

To investigate the phenomenon of peptide aggregation, a model peptide was selected (Figure 1). This peptide was selected since it has been previously studied [6]. Carbetocin is an analogue of a naturally occurring hormone, the cyclic peptide oxytocin. It has eight amino acid residues and is uncharged. There are both hydrophobic and hydrophilic properties of this peptide. The three most distinct hydrophobic side chains are, with their corresponding color and number from Figure 1, methyl-tyrosine (grey 8), leucine (red 2) and isoleucine (magenta 7). Apart from the peptide backbone there are side chains which allow for hydrogen bonding, glutamine (blue 6), aspartate (green 5) and glycine(NH2) (purple 1). Due to its ring-structure, the peptide backbone has reduced flexibility. A limited flexibility reduces the number of potential conformations and hence limits the number of ways the peptide can interact.

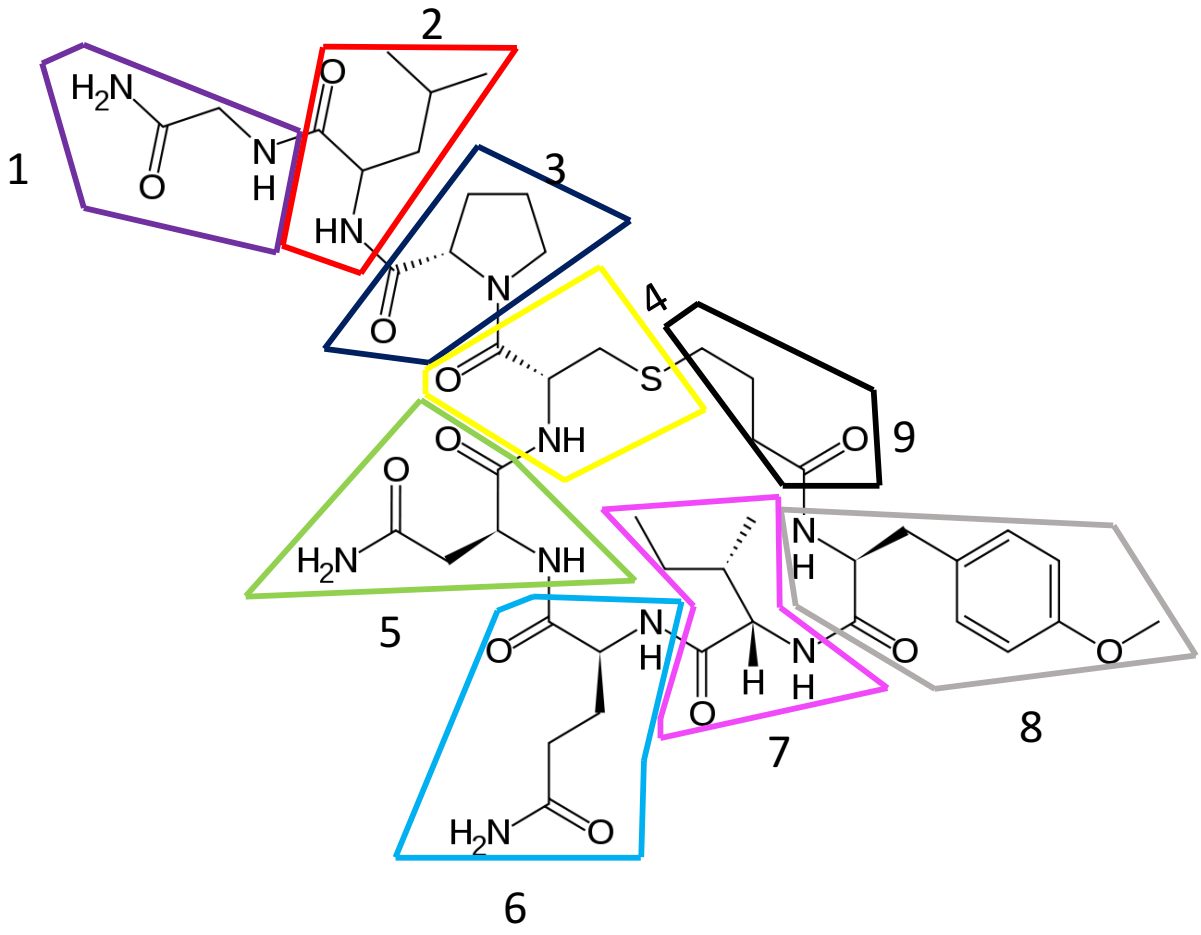

Figure 1: Carbetocin as a structural formula (bottom) and the full molecular structure (top) with indivudual amino acid residues: purple (1): glycine (NH2) – Gly(NH2), red (2): leucine - Leu, dark blue (3): proline -Pro, yellow (4): cysteine - Cys, green (5): aspartine - Asn, light blue (6): glutamine - Gln, magenta (7): isoleucine - Ile, grey (8): tyrosine(methyl) – Tyr(Me) and black (9): non-peptde bridge - Mba.

Carbetocin is used for treating post-partum hemorrhage (excessive bleeding after child-birth) by acting as an agonist on oxytocin receptors [21]. The current formulation of carbetocin is given as a 0.1 mg/ml injection and allows for a stability of 2 years when stored at 2-8 °C [4]. However, there are clinical trials (as of 2017) evaluating a new formulation which would allow for 3 years storage at 30 °C [6].

1.2 Surfactants

Surfactants (surface active agents) are amphiphilic molecules with both hydrophobic and hydrophilic properties which can self-assemble in solution or assemble at an interface. The general structure of a surfactant is often described as a hydrophilic head with a hydrophobic tail (Figure 2). In an aqueous solution, surfactants form self-assemblies called micelles, which are often spherical structures (other forms exist such as rod-like structures) with an oily interior composed of the hydrophobic tails and a hydrophilic exterior composed of the hydrophilic heads (Figure 2). A certain concentration of

surfactants is needed to form micelles, CMC is the critical micelle concentration, above which the concentration of monomeric surfactants practically does not increase [18].

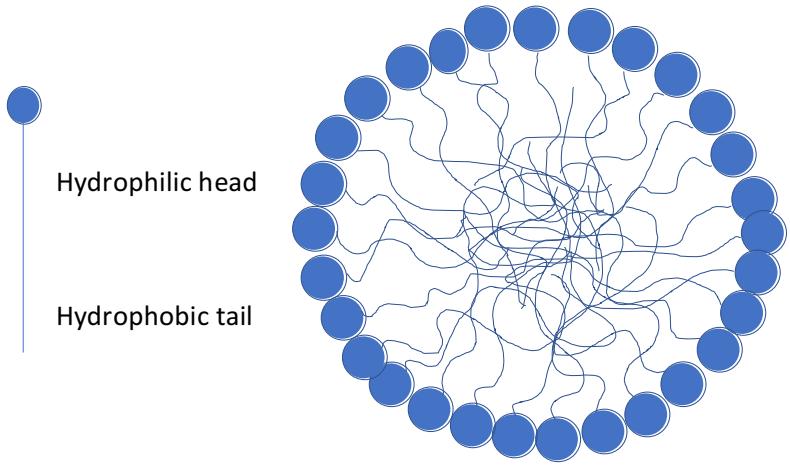

Figure 2: Schematic figure of a surfactant (left) and a cross-section of a micelle (right). Surfactants form micelles in which the hydrophobic parts are excluded from the aqueous surroundings.

Two surfactants were studied in this work, sodium dodecyl sulfate (SDS) and pentaethylene glycol monododecyl ether ($C_{12}E_5$) (Figure 3). These two surfactants have the same dodecyl tail but with different head groups. SDS is an ionic surfactant with a smaller head group whereas $C_{12}E_5$ is non-ionic with a longer polyethylene glycol (PEG) head group.

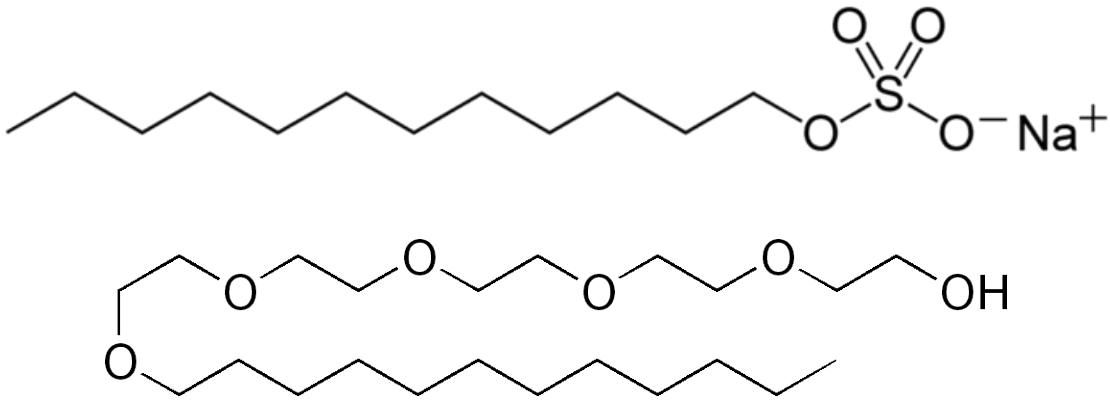

Figure 3: Top: sodium dodecyl sulfate (SDS). Bottom: pentaethylene glycol monododecyl ether ($C_{12}E_5$). These surfactants have the same dodecyl tail but with different head groups. SDS is ionic and the head group is smaller, whereas $C_{12}E_5$ is non-ionic with a longer head group.

Surfactants can be used in pharmaceuticals for several reasons: solubilizing of smaller drug molecules, by incorporating them into micelles, emulsifying agents, suspension stabilizers and wetting agents [3]. Concerning protein and peptide drugs, surfactants have e.g. been used as absorption enhancers when trying to develop oral formulations [22] and non-ionic surfactants have been used as aggregation inhibitors in some protein formulations [23]. The two surfactants used in this work were selected since they have the same tail and have been studied previously with carbetocin [6]. They are believed to give valuable insight to the aggregation mechanisms of carbetocin.

When peptides and surfactants are mixed, the aggregation of both species is affected [6][18]. Surfactants can form micellar structures on the polypeptide chain and hence lower the CMC, which is instead named critical association concentration (CAC) [18] and affect protein stability [23]. The peptide may also affect the micellar shape by disrupting the otherwise structured assembly. Additionally, surfactants may compete with the peptide for adsorption on surfaces and hence reduce aggregation [24] since adsorption can be an initiating step of aggregation [5].

1.3 Cyclodextrins

Cyclodextrins (CDs) are circular sugar molecules which form a cone-shaped structure with a hydrophobic cavity and a hydrophilic exterior due to the hydroxyl groups pointing outwards [25] (Figure 4).

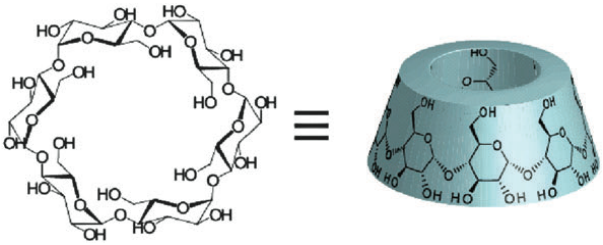

Figure 4: Structure of a typical cyclodextrin and a schematic of the 3D structure with a hollow interior [26].

This specific structure allows the CDs to form "guest-host complexes" with other molecules. The CD is the host and a hydrophobic guest molecule or a hydrophobic part of a molecule (such as a side chain of a polymer or peptide) is the guest inserted into the CD-cavity. The capturing of molecules in these cavities has several applications such as nano-sponges [25] and peptide drug delivery systems [27]. The interaction between the host and the guest is believed to be the hydrophobic interaction between the CD cavity and a hydrophobic part of the guest molecule and dehydration of the guest molecule, hence the hydrophobic effect [28]. There are many variants of cyclodextrins, in which some of the hydroxyl groups are substituted and rings of various sizes. In this work, methyl-ß-cyclodextrin (MBCD) was studied. It has previously been studied with carbetocin [6] and was therefore selected.

1.4 NMR spectroscopy

NMR (Nuclear Magnetic Resonance) spectroscopy is a commonly used technique within chemistry for analysis and characterization. In NMR spectroscopy, nuclei of molecules can be studied and information about how the atoms are connected and their chemical surrounding can be obtained. NMR spectroscopy uses the fact that some atomic nuclei, e.g. ^{1}H and ^{13}C, are magnetically active (or NMR active). By radiating a sample containing NMR active nuclei placed in a magnetic field, with a radiofrequency radiation, the nuclei (e.g. a ^{1}H nuclei = a proton) can get excited to a higher energy state. The relaxation of the nuclei spin (from a higher to a lower state) can be detected by a spectrometer [11]. It is these changes between spin states that is nuclear magnetic resonance [29]. Depending on the chemical connections and surroundings of the nucleus the peak(s) in the obtained spectrum will appear at different positions [30].

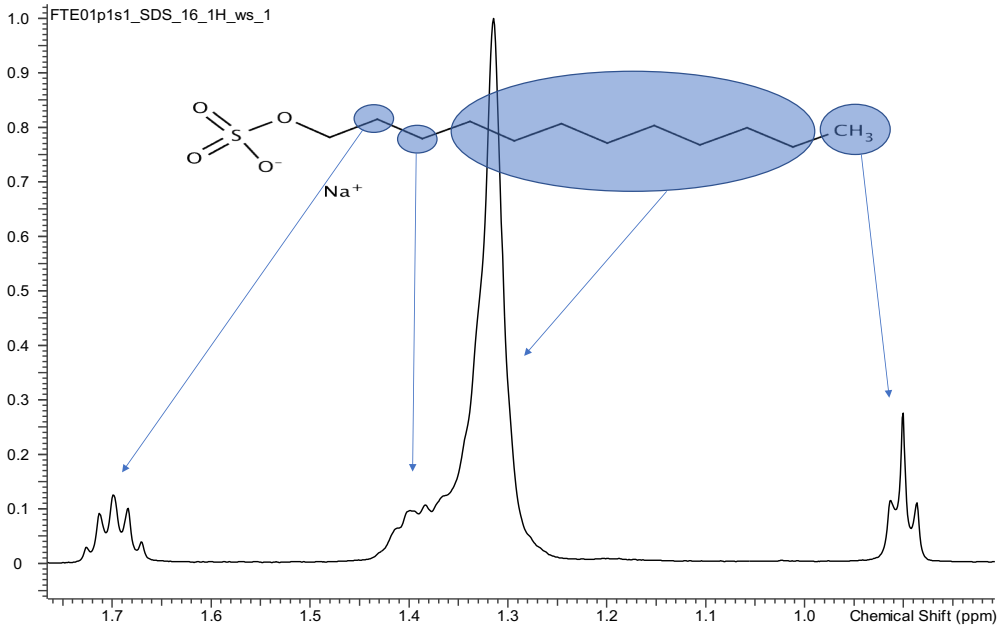

Figure 6: Part of the ^{1}H NMR spectrum of SDS showing peaks at different chemical shifts and with different splitting patterns. The protons from methyl group neighboring a CH_2 shows their distinct triplet splitting pattern at the far right of the spectrum. The alkyl chain protons produce the large peak in the middle and the two protons two carbons away from the oxygen give rise to the quintet at the far left. The peak from the protons closest to the oxygen is excluded from this image since they are far downfield in the spectrum

From an NMR spectrometer, a spectrum of frequencies (as in Figure 6) of the different nuclei's resonance frequencies is obtained. The NMR spectrum is often displayed as chemical shifts (δ) instead of frequencies, where a chemical shift is the relative frequency deviation from a reference substance, most often tetramethylsilane. Chemical shifts are measured in part per million (ppm) [30]. The δ depend on the magnetic field experienced by the nucleus. This magnetic field is sensitive to the nucleus' electronic environment: both the present bonding interactions and surrounding solvent [11], and hence equivalent nuclei will have the same chemical shift. An example of equivalent nuclei are the protons in methane or the middle part of the alkyl chain in SDS, Figure 5, and non-equivalent are for example the protons on different carbons in ethanol or the three groups of protons of SDS as highlighted in Figure 5. In Figure 6, displaying parts of the SDS ^{1}H NMR spectrum there are clear differences in chemical shifts for the different groups of protons. The methyl group in the SDS molecule has the lowest chemical shift (note the reverse scale on the x-axis) and a splitting pattern showing three peaks together, a triplet. This splitting pattern is typical for a methyl group neighboring a CH_2 group. The two equivalent protons in the CH_2 give rise to a triplet for the neighboring protons (CH_3). The three protons in the methyl group are equivalent and hence only one triplet is seen. A majority of protons in the alkyl chain cannot be distinguished and their corresponding peak is the big peak in the middle. The protons belonging to the peak with the highest chemical shift in Figure 5 are magnetically de-shielded by the nearby oxygen, in a way the others are too far away to be affected by, and hence get a higher δ. These protons are magnetically de-shielded since the oxygen decreases the electron density on the nearby nuclei due to its high electronegativity. The peak for the last two hydrogens closest to the oxygen are more magnetically de-shielded by the oxygen and are further downfield (to the left) in the spectrum, not shown in this example. Apart from the splitting patterns which allows for

chemical structure determination, conformational information can be obtained from an NMR spectrum. If the exchange between two conformations is fast, only one peak can be detected [31]. However, if it is slow, one peak for each conformation is seen with a separation of the size of their so-called coupling constant. A fast exchange may also lead to a broadening of the peaks. Changes in the appearance of the spectra and in the chemical shifts when SDS aggregates can be noted in Figure 7. In this figure, one spectrum displays SDS over its CMC value (red) and one is under (blue) and hence the red spectrum displays a more aggregated (micellar) solution. The peak furthest to the left has a lower chemical shift in the aggregated state and the peak in the middle has structurally changed compared to the less aggregated solution.

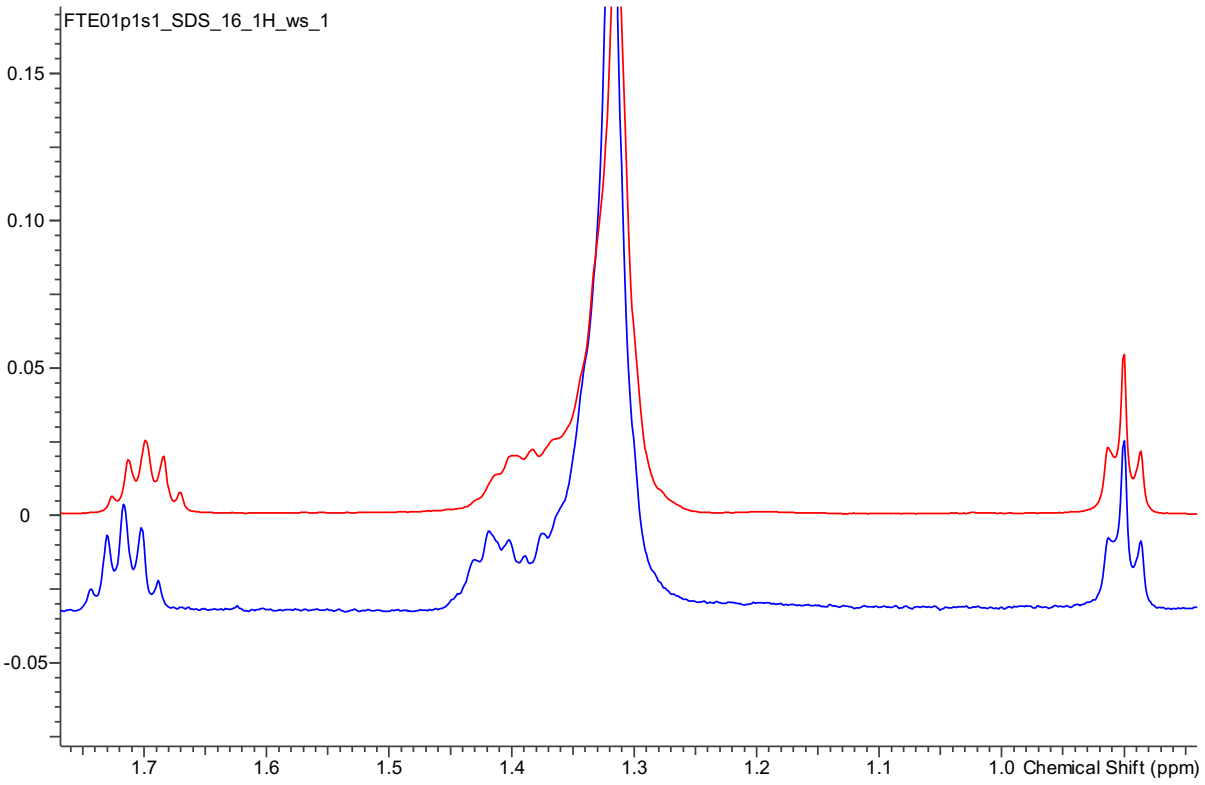

Figure 7: Part of the SDS ^{1}H NMR spectra for two concentrations, one above 16 mM (top in red) and one under 6 mM (bottom in blue) CMC. There are changes in the appearance of the spectrum. The peak in the middle has a different peak appearance and the peak to the left has a lower ppm value over CMC compared to under CMC.

When studying molecules with many non-equivalent protons, such as peptides, the spectrum becomes more complex with more peaks and diverse splitting patterns. As showed in the examples above, a lot of information about the molecules can be retrieved from an NMR spectroscopy experiment. When molecules aggregate, the surroundings and interactions with other molecules may change and NMR spectroscopy was therefore selected as the main method for this project.

There are many methods and variations of NMR experiments, below is a short introduction to the methods used in this project.

5.6.1 1D NMR

This is the standard NMR experiment. It can be done for all NMR-active nuclei and with an endless variety of settings and parameters depending on the information intended to be obtained. A spectrum

is obtained, such as Figure 6and Figure 7, showing the chemical shifts of the studied nuclei. It is considered 1D since there is only one frequency axis.

5.6.2 2D NMR

Correlates spins in two frequency dimensions. The spins can be either homonuclear spins (e.g. ^{1}H-^{1}H) or heteronuclear spins (e.g. ^{1}H-^{13}C). A 2D map of peaks is obtained, the peaks represent interaction between two nuclei. *J*-coupling is the interaction of the spins in nuclei connected via covalent bonds. The Nuclear Overhauser Effect (NOE) is another type of interaction in which the nuclei interact if they are close in space [30]. Depending on which experiment is used, interactions between nuclei at different distances and types are obtained.

COSY (COrrelation SpectroscopY) displays nuclei with J coupling. The spectrum displays peaks which correspond to nuclei that are J coupled [30].

HSQC (Heteronuclear Single-Quantum Correlation) identifies J couplings over just one bond length and hence directly connected nuclei produce peaks [29].

ROESY (Rotating-frame nuclear Overhauser Effect correlation SpectroscopY) displays NOE interactions and can hence identify spin couplings which are spatially close [29].

5.6.3 NMR Diffusometry and Diffusion

NMR diffusometry or diffusion-ordered NMR spectrometry (DOSY), referred to as dNMR in this report, is used to obtain information about the diffusion coefficient of different molecules/aggregates in solution. A series of spectra is obtained at different pulsed field gradient strengths and the decrease in the intensity of the spin echo signal is analyzed [29]. Depending on how much the molecule (or aggregate) moves between the different applied gradients, the signal is attenuated. The further it moves, the lower is the signal. This difference in signal intensity at different gradient strengths can be analyzed and diffusion coefficients can be obtained from the data [29]. The dNMR experiments in this work were performed with a stimulated echo sequence [32][33] where the following parameters are appropriately adjusted in order to obtain the diffusion coefficient. The delay between the gradient pulses (Δ), the width of the gradient pulses (w), the gradient strength (G), the measured signal intensity (I), the intensity with no gradient applied (I_0) and the gyromagnetic radius of protons (γ). With these values, the diffusion coefficient can be calculated through the Stejskal-Tanner equation [34]:

$$I = I_0 \exp\left(-D\gamma^2 G^2 w^2 \cdot \left(\Delta - \frac{\delta}{3}\right)\right) \qquad \text{Equation 1}$$

A stimulated echo sequence, instead of a standard spin echo sequence, was selected since the signals for solutions that are expected to aggregate or have large molecules will be attenuated in a standard spin echo experiment [32].

The diffusion coefficient D describes how fast a molecule (or other type of particle/aggregate) moves, the mean square displacement, in a solution due to Brownian motion. According to Stokes-Einstein's equation, the diffusion coefficient depends on temperature (T), viscosity (η) of the surrounding solvent and the hydrodynamic radius (r) of the moving species, as shown in Equation 2 [35]. k is Boltzmann's constant.

$$D = \frac{kT}{6\pi\eta r} \qquad \text{Equation 2}$$

Assumed in this equation is that the molecule is spherical. For non-spherical molecules/aggregates, the hydrodynamic radius is used. The hydrodynamic radius is defined as the radius of a sphere diffusing at the same rate as the non-spherical species [36].

6 Materials

Carbetocin (≥93%) was kindly donated by Ferring Pharmaceuticals. Sodium dodecyl sulfate (≥99.0%), pentaethylene glycol monododecyl ether (≥98.0%) and methyl-ß-cyclodextrin were purchased from Sigma Aldrich, sodium chloride (≥99.5%) and sodium iodide (≥99.5%) were from Merck, sodium sulfate (≥99.7%) from JT Baker, deuterium (≥99.8%) from Armar Isotopes. All water used for making solutions had been purified with a Millipore Milli-Q system.

7 Methods

7.1 Samples:

All samples were freshly prepared the same day or the day prior to the experiments. No D_2O or other deuterated solvent was added (as is common for NMR measurements) since as natural system as possible was preferred. D_2O is known to affect protein aggregation [37] which for obvious reasons was undesirable. With no deuterium in the samples, a lock signal cannot be obtained for any NMR measurements and hence drifting of the signals could be a problem. Early measurement provided spectra with good resolvable peptide peaks without a lock signal and hence the work proceeded with non-deuterated solvents. However, to obtain a decently uniform magnetic field, an automatic gradient shimming was used. Since all analysis was based on changes in chemical shifts relative to other samples, rather than absolute values, all results were assumed to be valid.

7.2 NMR:

After preparation, all samples were transferred with a pipette to 5 mm NMR tubes and the measurements were taken at 25°C. All dNMR measurements were performed on a Bruker AVII-200 spectrometer equipped with a Bruker DIFF-25 probe and a Bruker GREAT 1/40 gradient amplifier. The samples were inserted into the probe at least 15 min before measurement for temperature equilibration. A stimulated echo sequence was used with 32 gradient steps and 8 scans with a delay of 50 ms between the gradient pulses (Δ), a 1 ms width of the gradient pulses (δ) and the gradient strength (G) was linearly ramped in 32 steps. The sweep width was 2201 Hz, the acquisition time 1.0 s, the delay between scans was 2 s and the delay between the first two radiofrequency pulses was 2.12 ms.

All ^{1}H and 2D measurements (except from HSQC) were performed on a Varian Unity Inova 500 MHz spectrometer equipped with a Z-spec DBG500-5EF 5 mm dual broadband gradient probe. A water suppression (ws) sequence was used to suppress the otherwise dominating water peak for all ^{1}H measurements, this sequence has pulse widths of 11.8 and 23.6 μs. The following other parameters were used for the ^{1}H ws experiments: the sweep width was 8000 Hz, acquisition time 2.048 s, delay between scans 1.0 s and the number of scans was 4. ROESY was performed with water pre-saturation settings with a pulse width of 11.4 μs, a sweep width of 4262.6 Hz, acquisition time of 0.342 s, a delay of 2 s and 32 scans. For COSY the parameters were: pulse width of 11.4 μs, sweep width 4902 Hz, acquisition time of 0.3 s, a delay of 2 s and 8 scans.

All HSQC and ^{13}C measurements were performed on a Bruker Avance III 500 MHz with a Bruker SMART-Probe (bbo) and inserted at least 5 min prior measurement, the experiment was optimized for 145 MHz coupling and a relaxation delay of 1 s was used. ^{13}C measurements were performed in a ^{1}H

decoupled mode with and the number of scans was adapted to the concentration so that the signal to noise ratio would be approximately the same.

7.3 Viscosity

All viscosity measurements were performed on a 563 10 / I Ubbelohde viscometer from SI Analytics GmbH with a water bath setting the temperature at 25 °C. The samples were inserted at least 15 min prior to viscosity reading for temperature equilibration. The timing of the flowing liquid was done with a stop-watch and the viscosity was obtained through the instrument-provided equation, Equation 3. η is the viscosity and t is the time it takes for the liquid to flow between two marked lines on the viscometer.

$$\eta = 0.01033 \cdot t \qquad \text{Equation 3}$$

8 Results

8.1 Peak assignment

For analysis of NMR spectra, assignments of which peaks in the spectra belongs to which nuclei in the molecule are necessary. An almost complete assignment of carbetocin in dimethyl sulfoxide (DMSO) was provided by Ferring, not published results. Since DMSO and H_2O are different compounds, the NMR spectra of carbetocin in the two solvents will be different. NMR spectroscopy is sensitive to both a molecule's chemical interactions and surroundings. DMSO instead of H_2O could affect both, chemical interactions can change due to differences in hydrogen bonding between the peptide and the solvent and the surroundings obviously change when water is used instead of DMSO. Using the provided assignment along with ^{1}H and ^{13}C 1D NMR, $^{1}H^{1}H$ COSY, $^{1}H^{1}H$ ROESY and $^{1}H^{13}C$ HSQC 2D NMR, assignments for most of the carbetocin signals in H_2O were obtained Appendix 13.4. A table with all the peaks and their corresponding assigned ppm value is presented in Appendix 13.4.

8.2 Temperature dependence

It is known, as described in the introduction, that temperature can affect peptide aggregation. Experiments were performed to test the sensitivity to small differences in temperature for aggregation of carbetocin, the results were important for practical reasons (can we use different spectrometers and still compare the results) and for curiosity. The ^{1}H NMR spectra of carbetocin in water at different temperatures clearly showed a difference in chemical shifts even at one-degree difference, Appendix 13.2, and hence extra care for the temperature was taken when performing NMR experiments. NMR spectrometers can be temperature calibrated using a method described in Appendix 13.3.

8.3 Viscosity

Viscosity measurements can give insight to the behavior of a solution and hence potentially the aggregation behavior. These viscosity measurements were also performed due to that the diffusion coefficient is dependent on the viscosity of the solvent. For solutions with well-structured aggregates such as micellar solutions, the solvent viscosity is generally not affected by viscosity changes of the bulk solution. The system can be seen as that the micelles affect the bulk viscosity but not the viscosity in between the micelles [personal communication]. Hence the viscosity of the solvent for aqueous surfactant solutions is seen as 0,89 mm^2/s which is the same as for water at 25 °C [38]. However, for solutions in which the solute form non-structured aggregates which are more like a network of molecules, the viscosity of the solvent is seen to have changed and is no longer the same as the viscosity of water/solvent. These differences are not distinct and how the viscosity of the bulk solvent changes is gradual. Viscosity measurements of carbetocin and additives are presented in Table 1:

Table 1: Kinematic viscosity of carbetocin and additives. Values are averaged of three runs made on each sample.

Sample	Kinematic viscosity (cm^2/s) at 25 °C	Run 1 (s)	Run 2 (s)	Run 3 (s)
Carbetocin 47 mM	1.08	105	104	105
Carbetocin 14 mM	0.940	91	91	91
Carbetocin 5.05 mM	0.908 *	-	-	-
Carbetocin 5.05 mM + MBCD 126.5 mM	1.56*	-	-	-
SDS 225 mM	1.61	157	158	154
SDS 225 mM + carbetocin 15 mM	1.65	160	160	160
SDS 45 mM + carbetocin 15 mM		89	89	89
SDS 15 mM + carbetocin 15 mM	1.02	99	99	99
SDS 15 mM	0.919	89	88	88
$C_{12}E_5$ 15 mM + carbetocin 15 mM	1.01	98	97	98
$C_{12}E_5$ 15 mM	1.33	128	127	130

* Provided by Ferring, not published

8.4 Diffusion NMR

This project actually started with results from previous studies (not published [personal communication]) obtained through dNMR, suggesting that carbetocin aggregation increases with concentration. In this early work only three peptide concentrations were used, and hence to further show that aggregation does occur for carbetocin, dNMR was performed for a more extensive concentration series of aqueous carbetocin. The results from these dNMR experiments are presented in Figure 8. Since the nature of the carbetocin aggregates is not well-defined, or rather not known, it is not clear if the viscosity of the solvent has changed, as described in 8.3. The normalization was performed under the assumption that the viscosity is unaffected by the density which allows for the switching between the kinematic viscosity obtained in this work and the dynamic viscosity which is used when calculating the diffusion coefficient. Additionally, a linear relationship between concentration and viscosity was assumed. The diffusion coefficients (D) were obtained through Equation 1 after a least-square fitting to the dNMR data. The experimental values (the intensity) were obtained through an integration of a selected peak in the carbetocin spectrum.

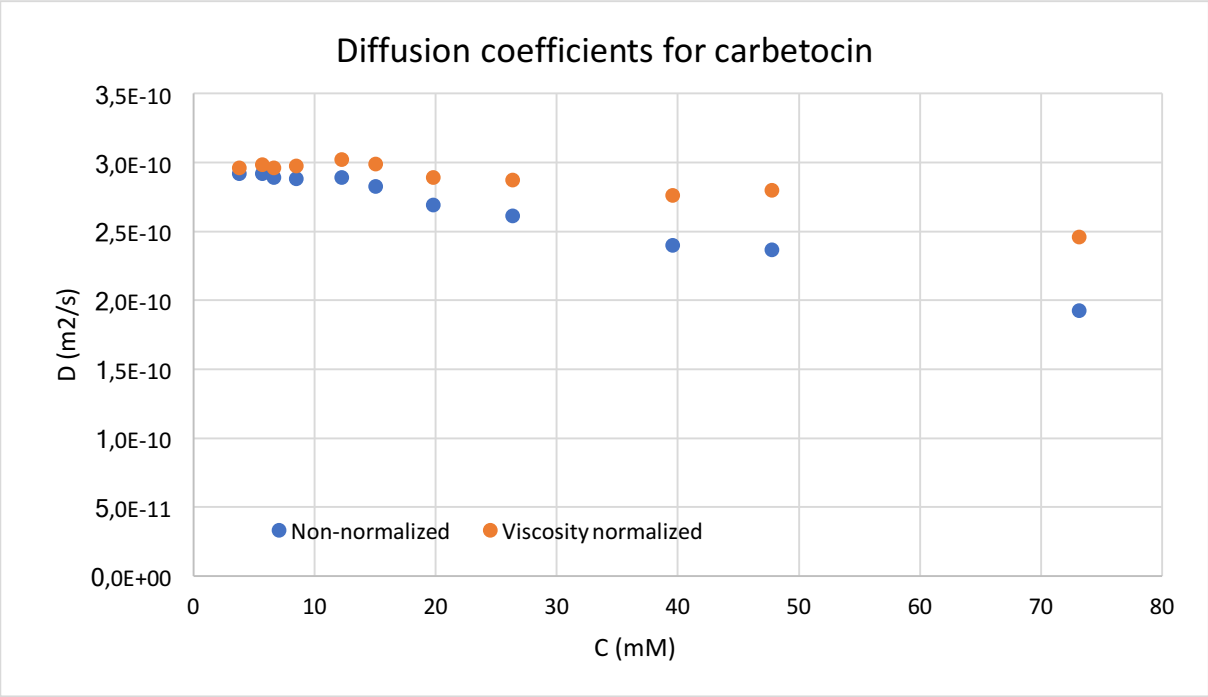

Figure 8: Diffusion coefficient (D) of different concentrations of carbetocin in water. First above a concentration of around 15 mM is a decrease in D observed. Orange dots represent viscosity normalized data and blue are not normalized for viscosity.

The same trend is noted for both the normalized and the non-normalized data, there is a clear trend within the higher concentrations (> 15 mM) (Figure 8), there is a decreasing D with increasing concentration. However, for the lower concentrations (≤15 mM), D is practically unchanged with varying concentrations. The observed diffusion coefficients (D_{obs}) are the weighted average of all the possible formations of molecules/aggregates in the sample. Aggregates of various sizes, dimers, hexamers etc. will have different diffusion coefficients (D_i) depending on their size, monomeric molecules will have yet another value. D_{obs} can hence be described with Equation 4.

$$D_{obs} = \alpha_1 D_1 + \alpha_2 D_2 + \alpha_3 D_3 \ldots \quad \text{Equation 4}$$

α_i is the fraction of carbetocin with the specific D_i.

The hydrodynamic radius was calculated from Equation 2, with $D=D_{obs}$ of the non-normalized data (Table 2). There is an increasing radius with increasing carbetocin concentration.

Table 2: Hydrodynamic radius of carbetocin aggregates in different carbetocin concentrations

Carbetocin concentration (mM)	Hydrodynamic radius (nm)
73.1	1.27
47.7	1.04
39.5	1.02
26.4	0.910
19.8	0.910
15.0	0.867
12.2	0.848
8.47	0.851
6.59	0.848
5.65	0.839
3.77	0.839

8.5 Concentration series of aqueous carbetocin

8.5.1 ^{1}H NMR

To further analyze aggregation of carbetocin, ^{1}H NMR spectroscopy was performed on a concentration series of carbetocin in aqueous solution, 5 to 73 mM. We wanted to see if the same trends from dNMR results would show also in ^{1}H NMR results, since ^{1}H NMR spectroscopy provides information about chemical interactions and molecular surroundings, which are believed to change when aggregation occurs. Parts of the spectra showing the largest changes in the appearance of the spectra between the different carbetocin concentrations are showed in Figure 9. A distribution along the concentration series has been selected with highest concentration at the top spectra and lowest at the bottom.

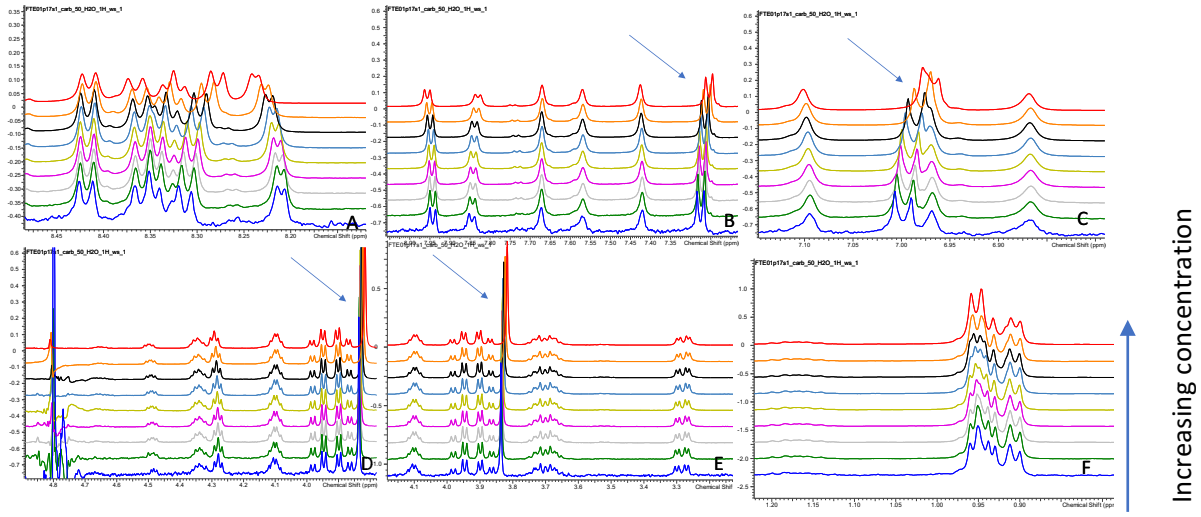

Figure 9: ^{1}H NMR spectra of different concentrations of carbetocin in water, the top line refers to the highest concentration and the bottom line is the lowest concentration. The different boxes are different parts of the spectra showing sites were clear changes between the concentrations can be noted. The chemical shifts of some peaks change, some to a lower and some to a higher ppm value. Note also the shape differences of some peaks when going from a lower to a higher peptide concentration. A: amide protons showing significant changes in both shape and chemical shifts. B & C: The peaks with the arrows belong to the tyrosine side chain, clear change in chemical shift on both. D & E: The peak with the arrow belongs to the tyrosine side chain and shows a clear change in chemical shift. F: Peaks from the methyl groups of leucine and isoleucine showing a shape change with different concentrations.

The appearance of some peaks changes and the chemical shifts of many peaks change (change in chemical shift = Δδ). The changes are not large when comparing absolute ppm values, however, there are clear trends to be detected. The most significant changes are for the amide hydrogens in the backbone of the peptide (Figure 9 A) and for the changes of the tyrosine residue (Figure 9 B, C and D) (also in E same peak as in D). The peaks belonging to the tyrosine residue are marked with arrows. Another clear change in peak pattern appearance is for the methyl groups of leucine and isoleucine (Figure 9 F) with increasing concentration the peaks go from a triplet and a singlet to a doublet and a singlet.

The Δδ, relative to the chemical shifts for the lowest concentration analyzed in this work (5mM) of carbetocin, are plotted for peaks showing a large change (Figure 10). Three of five of the peaks with the largest Δδ (at 47 mM carbetocin compared to the 5 mM sample) belong to Tyr(Me), the other two belongs to amide protons in the backbone of the leucine and glutamine. The amide in the glycine residue has the sixth largest Δδ. In Figure 10, a clear increase in Δδ with increasing carbetocin concentration is observed for all these selected peaks. The other peaks follow the same trend, however not to the same degree, Δδ relative to the 5 mM sample for all peaks are plotted and tabulated in Appendix 13.5. Appendix 13.5 displays the Δδ values for all ^{1}H NMR peaks with the two different reference peaks as well, since there is no lock signal from a deuterated solvent or other reference peak in the samples, a reference peak has been chosen to prevent misinterpretations from potential drifting of the chemical shifts. The results in this section, have the peak with the lowest ppm (methyl groups from Leu and Ile) set as reference. When another reference (βH2Gln) was used, there were some changes, however the same trend of the tyrosine residue having the largest Δδ along with backbone amide protons were observed.

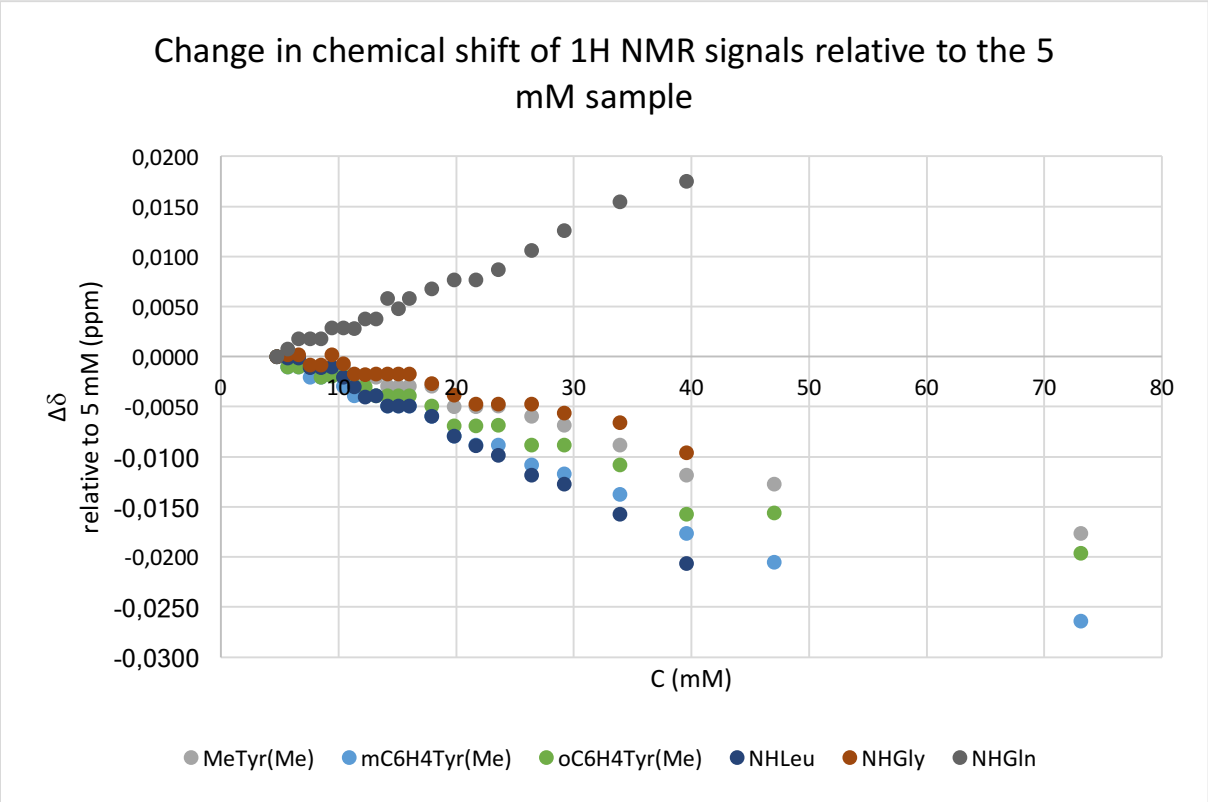

Figure 10: Δδ of a carbetocin concentration series relative to a 5 mM carbetocin sample. Larger changes for higher concentrations.

8.5.2 ^{13}C NMR

The same trend as for the ^{1}H spectra is observed in the ^{13}C spectra, and the same side chains show the largest change in chemical shift. However here the largest Δδ (of the 50 mM samples compared to the 6 mM sample) belong to all the carbonyl carbons in the backbone. When studying the amino acid side chains, the same trend as for the ^{1}H spectra is observed; the tyrosine residue shows the largest Δδ. A plotted diagram of all peaks' Δδ from the ^{13}C NMR experiments is found in Appendix 13.5**.**

8.6 Cyclodextrin

^{1}H NMR and dNMR were performed on MBCD-carbetocin samples, Appendix 13.6. Clear changes can be noted in the ^{1}H NMR spectra, similar changes as in Figure 9 C and D of when the carbetocin concentration increases can be noted. These results suggest that aggregation of carbetocin increases in the presence of MBCD or that the interaction between the two molecules is similar to the self-interaction of carbetocin. The dNMR results were hard to interpret, partly because of the viscosity increase of the solution with increasing MBCD concentration, and no replications of experiments were performed since focus was decided to be on surfactant and carbetocin interaction. Hence the results are only presented in the appendix and will not be further evaluated. Although, it can be said that MBCD and carbetocin most likely interact and form co-aggregates.

8.7 Surfactants

^{1}H NMR and dNMR experiments were performed on SDS-carbetocin and $C_{12}E_5$-carbetocin samples for further analysis of how carbetocin aggregates and how these additives affect the aggregation behavior.

8.7.1 SDS

dNMR and ^{1}H NMR was performed on SDS-carbetocin samples with various SDS concentrations and a constant carbetocin concentration of 15 mM. The obtained diffusion coefficients are presented in Figure 11. The diffusion coefficients for SDS are practically the same for all concentrations above the CMC of 8 mM (7-8 $\cdot 10^{-8}$ m^2/s), below CMC the diffusion coefficient is higher ($1.4 \cdot 10^{-10}$ m^2/s). For carbetocin, the diffusion coefficients decrease with increasing SDS concentration. Note the difference between 15 mM SDS with and without carbetocin. Without carbetocin, the D is $3.6 \cdot 10^{-10}$ m^2/s and with it is $8.6 \cdot 10^{-11}$ m^2/s. Also worth noting that the reference value for carbetocin 15 mM is $2.84 \cdot 10^{-10}$ m^2/s which is higher than all D values of when SDS is present in the 15 mM carbetocin solutions.

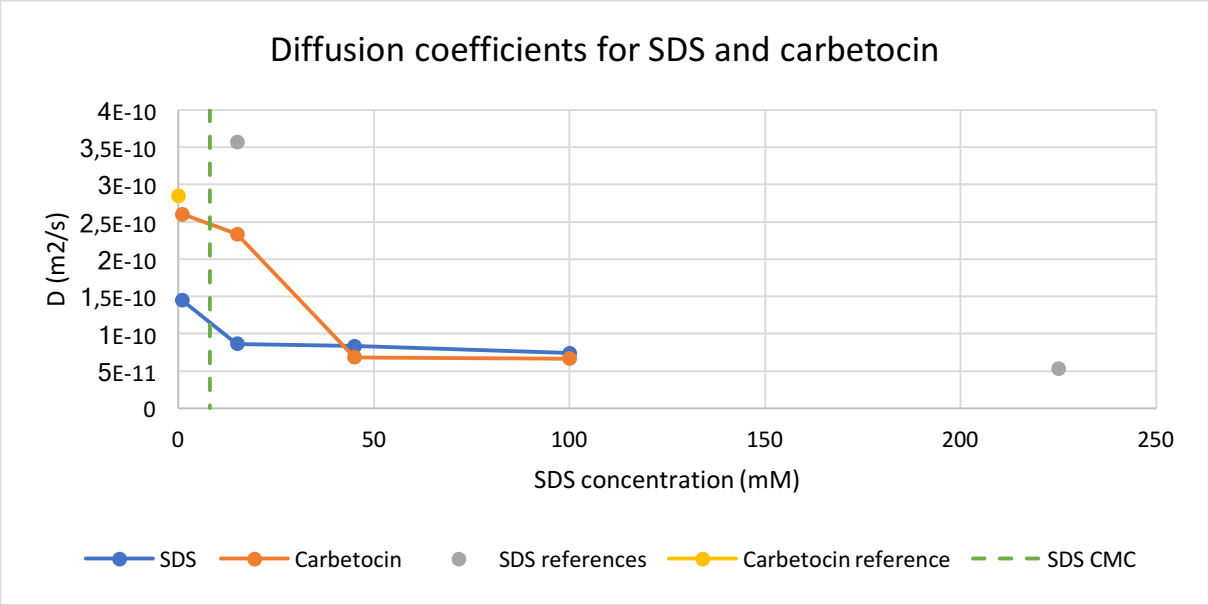

Figure 11: Diffusion coefficients of SDS and carbetocin of SDS-carbetocin solutions. Carbetocin concentration constant at 15 mM and SDS in an increasing concentration from 1 to 225 mM. Carbetocin in orange and SDS in blue. Reference diffusion coefficients for both SDS (15 and 225 mM) and carbetocin (15 mM) are displayed in grey respectively yellow. CMC of SDS (8 mM) is marked with a green dashed line.

Figure 12 shows a part of the ^{1}H NMR spectra of carbetocin and SDS solutions, with different SDS concentrations. In all samples, except from the 15 and 225 mM SDS references, there is 15 mM carbetocin and the SDS concentrations are 1, 15, 45 and 100 mM. There is additionally a reference sample of 15 mM carbetocin without SDS. Apart from the peaks originating from the SDS molecules, there are other differences between the samples containing SDS and the carbetocin reference. The peaks are clearly broader in the carbetocin-SDS spectra. The spectrum with the broadest peaks is the sample with a SDS concentration of 15 mM i.e. at a molar ratio of SDS to carbetocin of 1. It is also for this sample that the methylated tyrosine methyl peak at around 3.8 ppm has the largest $\Delta\delta$ (0.11 ppm lower value) compared to the reference carbetocin sample.

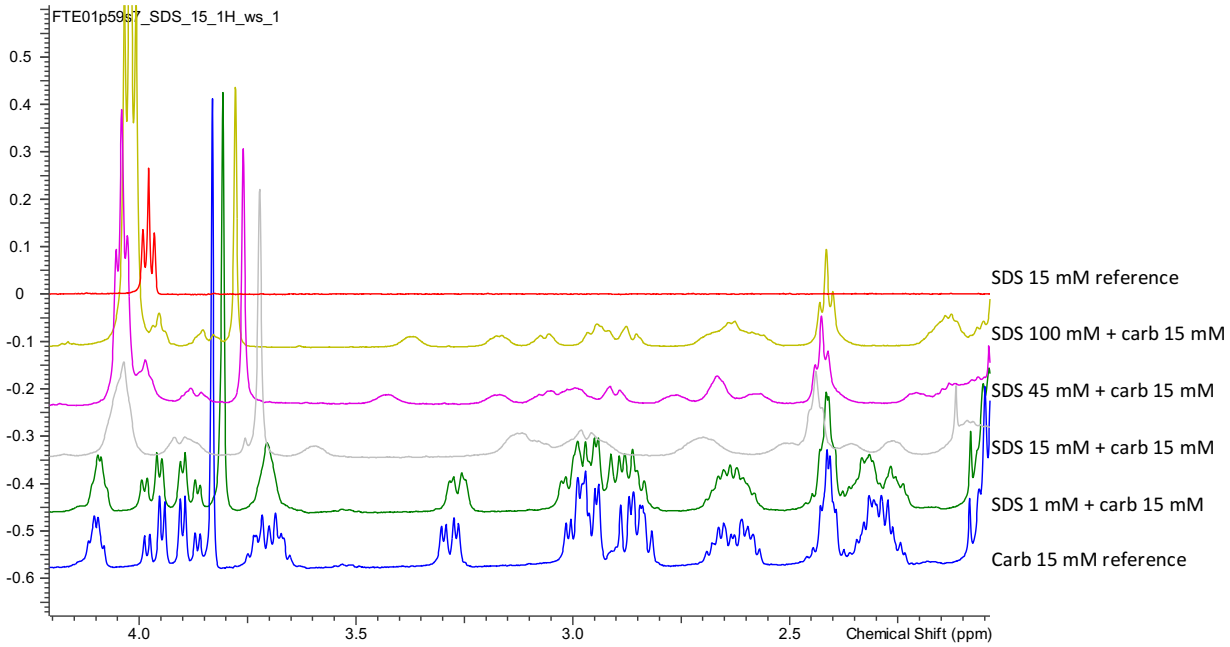

Figure 12: 1H NMR spectra for a concentration series of SDS in 15 mM carbetocin, a reference sample of carbetocin at the bottom (blue). Note the changes in the appearance of the spectra, chemical shifts, peak appearance and broadening of the peaks. From the top red: 15 mM SDS (reference), yellow: SDS 100 mM and carbetocin 15 mM, purple: SDS 45 mM and carbetocin 15 mM, grey: SDS 15 mM and carbetocin 15 mM, green: SDS 1 mM and carbetocin 15 mM and blue: carbetocin 15 mM (reference).

8.7.2 $C_{12}E_5$

dNMR experiments were performed on $C_{12}E_5$-carbetocin samples with various $C_{12}E_5$ concentrations. The obtained diffusion coefficients are presented in Figure 13**.** The diffusion coefficients decrease both for carbetocin and $C_{12}E_5$ with increasing $C_{12}E_5$ concentration. Note the difference between 0.12 mM $C_{12}E_5$ with and without carbetocin. With carbetocin it is $1.8 \cdot 10^{-10}$ m^2/s and without it is $1.4 \cdot 10^{-10}$ m^2/s. For 15 mM $C_{12}E_5$ with and without carbetocin they are $4.4 \cdot 10^{-11}$ m^2/s respectively $1.3 \cdot 10^{-11}$ m^2/s.

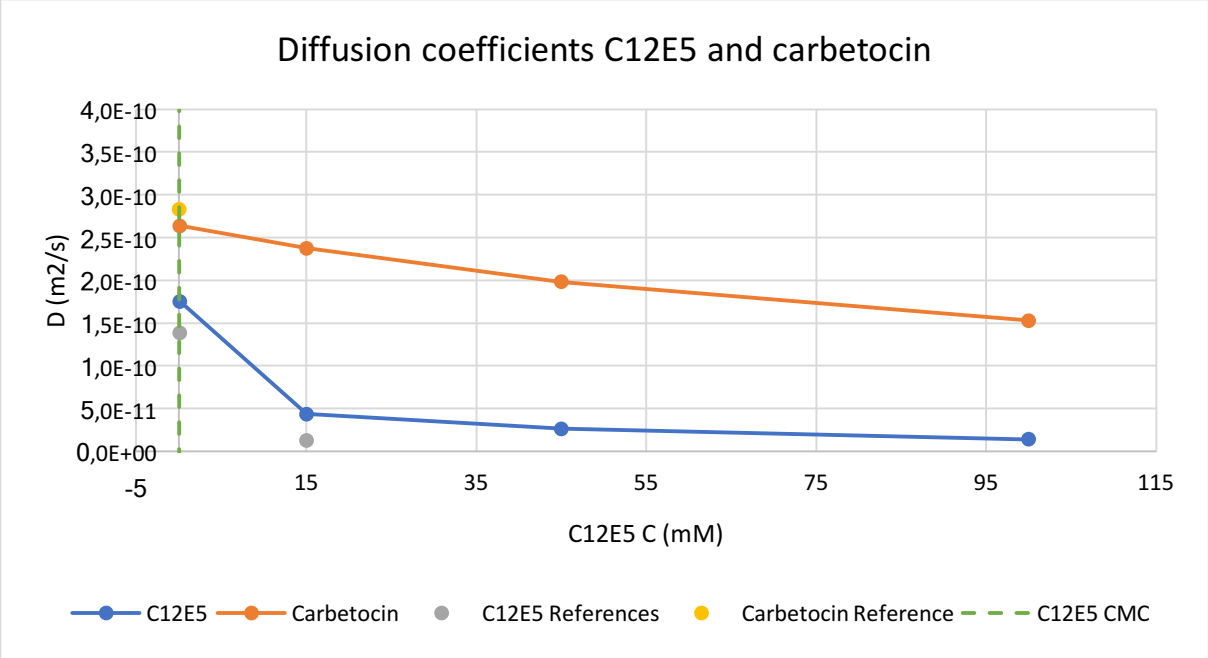

Figure 13: Diffusion coefficients of $C_{12}E_5$ and carbetocin of $C_{12}E_5$-carbetocin solutions. The carbetocin concentration was constant at 15 mM and $C_{12}E_5$ in increasing concentrations. Carbetocin in orange and $C_{12}E_5$ in blue. Reference diffusion coefficients for both $C_{12}E_5$ (0.12 and 15 mM) and carbetocin (15 mM) are displayed in grey respectively yellow. CMC of $C_{12}E_5$ (0.06 mM) is marked with a green dashed line.

Figure 14 shows a representative part of the ^1H NMR spectra of a $C_{12}E_5$ concentrations series of carbetocin-$C_{12}E_5$ solutions. In all samples, there are 15 mM carbetocin and the $C_{12}E_5$ concentrations are 0.12, 15, 45 and 100 mM. There are also a references samples of 15 mM carbetocin and 15 mM $C_{12}E_5$. Differences between the concentrations were most clearly seen downfield, where amide protons and aromatic protons have their signals, and hence this part of the spectra is highlighted in the bottom of Figure 14.

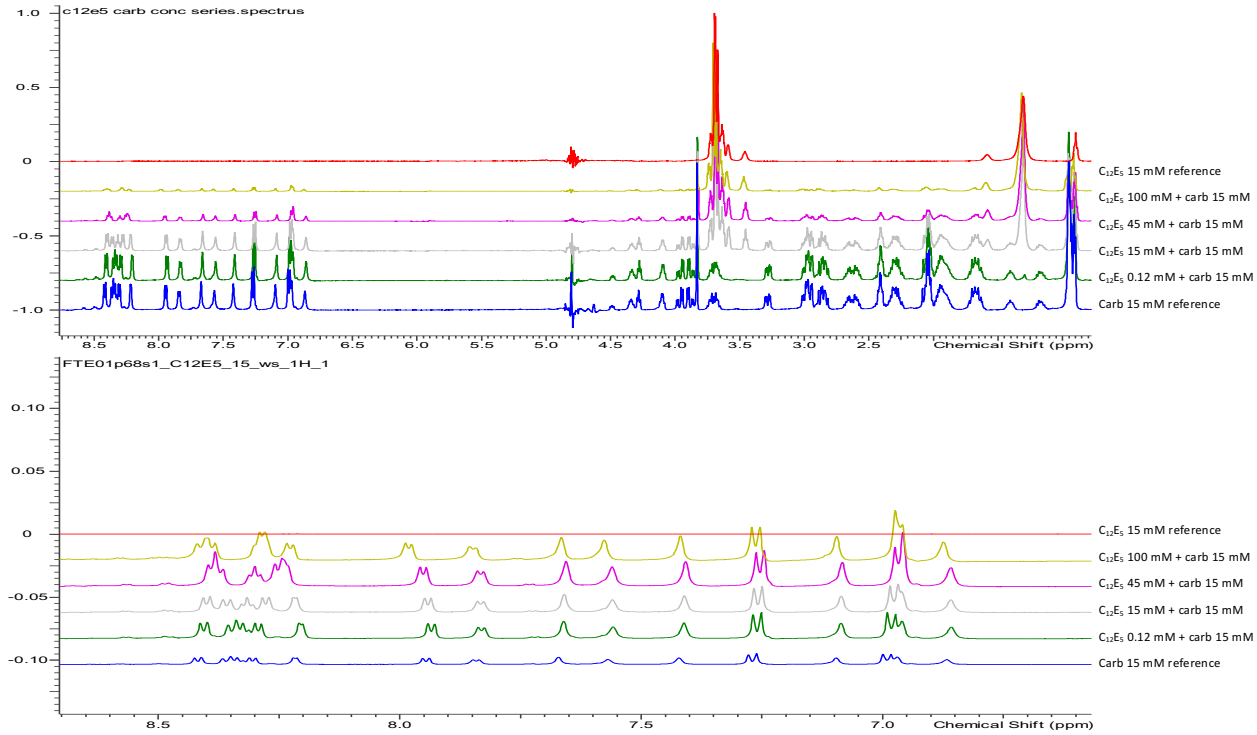

Figure 14: 1H NMR spectra for a concentration series of $C_{12}E_5$ in 15 mM carbetocin and a reference sample of carbetocin at the bottom (blue).From the top, red: $C_{12}E_5$ 15 mM (reference), yellow: $C_{12}E_5$ 100 mM and carbetocin 15 mM, purple: $C_{12}E_5$ 45 mM and carbetocin 15 mM, grey: $C_{12}E_5$ 15 mM and carbetocin 15 mM, green: $C_{12}E_5$ 0.12 mM and carbetocin 15 mM and blue: carbetocin 15 mM (reference).

9 Discussion

9.1 Carbetocin

From the diffusion coefficients results, (Figure 8), it is clear that the carbetocin molecules/aggregates at the higher carbetocin concentrations on average have lower D and hence on average are larger than the ones in the lower concentrations. When plotting the dNMR data against the inverse concentration (Figure 15), a trend becomes clear. A distinct decrease in diffusion coefficient is noted for concentrations above around 15 mM, whereas there is no notable variation for the lower concentrations. Analyzing this system as a two-state system where the molecules either are in monomeric form or in aggregated form (similar to how surfactants either are free in solution or reside in micelles), one can describe the behavior by Equation 5 [18], hence the use of the inverse concentration in the figure.

$$D_{obs} = \frac{c_{mono}}{c} D_{mono} + \frac{c_{agg}}{c} D_{agg} \qquad \text{Equation 5}$$

D_{obs} is the observed diffusion coefficient, D_{mono} is the diffusion coefficient for monomeric molecules, D_{agg} is the diffusion coefficient for aggregates (assuming all aggregates have the same D), c is the total concentration and $c_{mono/agg}$ is the concentration of monomers respectively aggregates. If a system follows Equation 5, one should see two straight lines intersecting at the CMC (or CAC) [39]. In Figure 15 this behavior can be seen, and the lines are intersecting at around 0.055 mM^{-1} (18 mM) indicating that this would be the critical concentration for which carbetocin aggregates. However, when using this model, one assumes that only one type of aggregate forms and from the results in this work, it is not clear if this is the case, since the structure of the carbetocin aggregates is not known. These results do indicate that something happens to solutions of >18 mM carbetocin which could be worth to investigate further. A concentration series of more samples around this potentially critical concentration would be able to determine more exactly where this critical point could be and give a better idea of the possible curvature of the dashed line in the dependence of c^{-1}, Figure 15. The fact that there is an indication of a curvature implies that this two-site system model is not good enough in describing the system of carbetocin aggregation. Further studies would allow for the development of an alternative model.

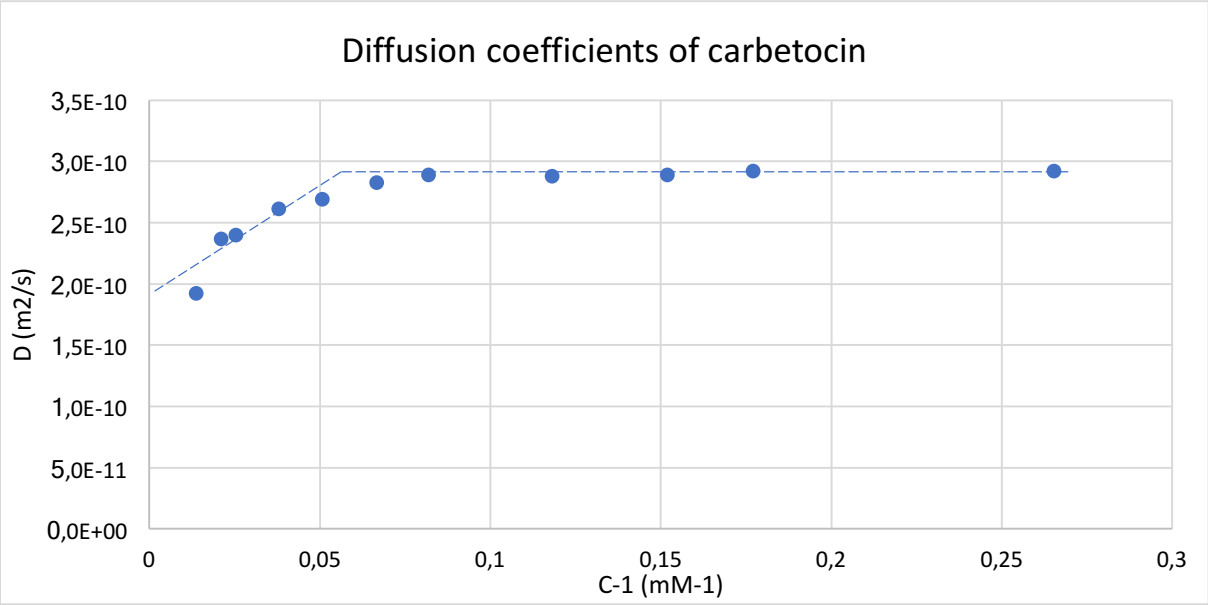

Figure 15: Diffusion coefficients of carbetocin in H_2O related to carbetocin concentration. Note the inverse concentration on the x-axis. A clear decrease in diffusion coefficient value for higher carbetocin concentrations. There are no clear differences in D for the lower carbetocin concentrations. The distinct decrease in D starts >18 mM carbetocin. Dashed line represents the two-site system described by Equation 5.

From the 1D NMR experiments, changes in chemical shifts, with a practically linear dependence on concentration, are detected at all concentrations. Without the dNMR results, this trend could be thought to be due to the change in surroundings of the molecule which occurs when the carbetocin concentration increases and hence changing the character of the bulk solution. With the dNMR results, showing an increase in aggregation with increasing carbetocin concentration, however, it is strongly suggested that the trend in ^{1}H NMR spectra also has to do with aggregation. It could be that aggregates are forming already at these lower concentrations even though they are not detected in the dNMR measurements.

However, in the ^{1}H NMR, there are changes in chemical shifts already at the lower concentrations, compared to changes seen only for higher concentrations in the dNMR results. This can be explained by the Stokes-Einstein equation, Equation 2. The diffusion coefficient is dependent on the hydrodynamic radius of the molecule/aggregate, as described in section 5.6.3, and it could be that the hydrodynamic radii of the aggregates formed at lower concentrations do not change significantly compared to the monomeric form, and hence no difference is seen in the dNMR data. As schematically showed in Figure 16, the hydrodynamic radius of an oblate-formed molecule (which carbetocin possible could be) and an aggregate of two such molecules might be the same. Hence, from the dNMR results, these two would not be possible to distinguish, but the ^{1}H NMR shows a difference since the two molecules in the dimer are interacting. ^{1}H NMR is sensitive to both chemical interactions and molecular surroundings and an interaction shown in Figure 16 could affect the ^{1}H NMR spectrum of carbetocin.

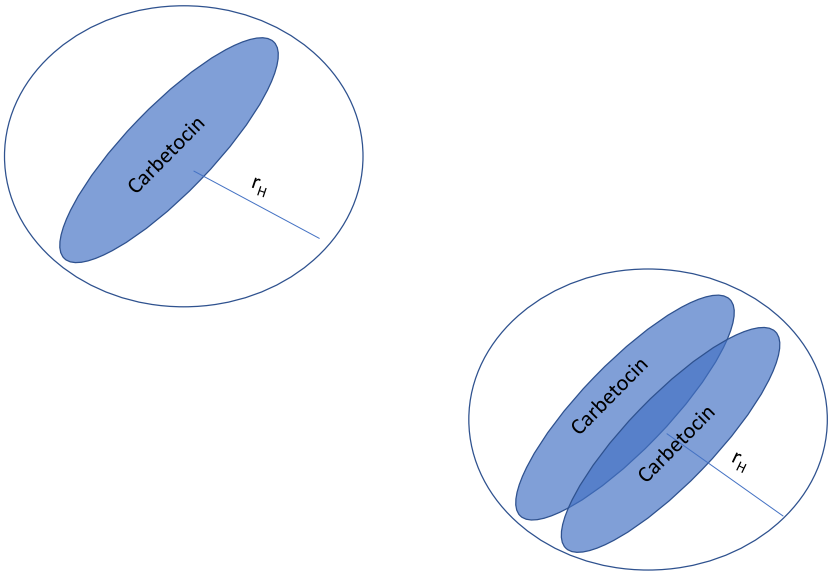

Figure 16: Schematic presentation of a monomeric carbetocin with hydrodynamic radius of r_H and a dimer of carbetocin with a hydrodynamic radius of the same length, r_H.

A change in chemical shift may be due to various reasons, of which the following are considered in this work: change in the electronic surroundings (such as changes in hydrogen bonding or hydrophobic interactions) and a shift in molecular conformation. The ^{1}H and ^{13}C NMR data showed that the tyrosine residue had the largest $\Delta\delta$ (of the 47 mM sample relative to the 5 mM sample) of the side chains. The $\Delta\delta$ increased with carbetocin concentration. This suggests that the tyrosine residue is involved in the aggregation of carbetocin. Tyrosine is considered to have a hydrophobic side chain and with the extra methyl group creating Tyr(Me), which is the residue present in the carbetocin molecule, it becomes even more hydrophobic. Accordingly, the PPIs causing the aggregation probably consists of (at least partly) hydrophobic interactions. This is in line with previous literature describing that PPIs often involves hydrophobic interactions [6]. From the ^{13}C results, the carbons with the largest $\Delta\delta$ (of the 47 mM sample relative to the 6 mM sample) were the carbonyl carbons in the peptide backbone. The carbonyl oxygens have a partial negative charge due to the difference in electronegativity with carbon and can thus act as a hydrogen bond acceptor. A change in the hydrogen bonding of the carbonyl oxygen (the forming or cleaving of hydrogen bonds) affects the chemical shifts of the carbonyl carbon [39]. A change in the chemical shifts of the carbonyl carbons were seen in the ^{13}C NMR results (Appendix 13.5) and the ^{1}H NMR results (Figure 10) show that some of the amide protons in the peptide backbone have relatively large $\Delta\delta$, indicating that these would be the hydrogen-donors in the peptide-peptide hydrogen bonding. These results suggest that hydrogen bonding together with hydrophobic forces are dominant in the PPIs of carbetocin aggregation.

Results here show that the tyrosine and backbone peaks have the largest $\Delta\delta$ (Figure 10). This does not directly prove that the nuclei connected with these peaks are affected the most by the aggregation, although it strongly indicates that these are affected in some degree. However, these results, that the hydrophobic residue has large $\Delta\delta$ along with previous knowledge that hydrophobic interactions are important in peptide aggregation, suggest that these peaks showing large $\Delta\delta$ do have a major role in the aggregation of carbetocin.

9.2 Carbetocin with surfactants

Since carbetocin most probably interacts partly with hydrophobic forces in self-aggregation, it is believed that the same interactions would be present as well in carbetocin-surfactant interactions. When observing the ^{1}H NMR spectra of SDS-carbetocin samples (Figure 12), clear changes can be noted that are similar to how the spectrum changes when aggregation occurs in the carbetocin samples with no additives (the peak corresponding to the tyrosine residue is shifting upfield). These changes indicate that carbetocin self-aggregation increases when SDS is added, or more likely, that the same residues involved in carbetocin self-aggregation are involved in the SDS-carbetocin interaction. According to Høgstedt et al. [6], the tyrosine residue is not involved in the SDS-carbetocin interaction. In their study, they have used near-UV circular dichroism as an analytical method which is a method analyzing aromatic parts of molecules, and there were barely any changes between the carbetocin sample containing SDS and the one without. These contradictory results suggest that further research on the matter is needed to conclude whether the tyrosine residue of carbetocin is involved in the carbetocin-SDS interaction or not. However, the results from this previous study, can be interpreted as the tyrosine residue being involved in similar ways between the self-aggregation of carbetocin and the co-aggregation between SDS and carbetocin.

The dNMR results (Figure 11), suggest that the aggregates formed are of mixed character, containing both SDS and carbetocin molecules since the diffusion coefficients for both SDS and carbetocin are decreasing compared to their reference values when in a mixed solution.

An interesting result is the ^{1}H NMR spectrum of 15 mM SDS in 15 mM carbetocin (Figure 12). This spectrum contains the largest $\Delta\delta$ (0.11 ppm) of all SDS samples for the peak at 3.8 ppm, relative to the reference sample of only carbetocin. Additionally, this spectrum has the broadest peaks of all SDS-spectra. A broadening of peaks may in this case be due to at least two different mechanisms. One is due to a slower exchange between two components that individually would give rise to two individual signals, in this case monomers and aggregates. It is possible that the exchange between monomeric carbetocin and carbetocin co-aggregated with SDS is slowest for a molar ratio of 1. However, the lifetime of the aggregates (if a slower exchange is the reason for the broadening) must be quite long and normally the lifetime of micelles is relatively short, hence, what is believed to be the cause in this case is the reduced mobility of the studied molecule/aggregate. A bigger aggregate has less mobility and hence would give rise to broader peaks because of the shorter T_2 relaxation. The broadening in Figure 12 is believed to come from that the aggregates in SDS concentration of 15 mM give rise to the largest aggregates. One could imagine that without carbetocin present, the surfactants form spherical micelles, but when carbetocin is added, it disrupts the spherical structure and larger micelles of other forms are formed: e.g. rod-like structures or spherical with carbetocin pointing outwards creating a bulky structure**.** In the lower SDS concentration (1 mM), barely any SDS molecules are in micelles since the concentration is well below CMC and hence the mobility of the molecules/aggregates are not affected significantly. At the higher SDS concentration (100 mM), a large extent of the SDS molecules will reside in micelles since the concentration is more than ten times CMC, but the carbetocin concentration is low in comparison and hence there will not be enough carbetocin molecules to affect the micellar shape and size to a degree that can be noted in a ^{1}H spectrum as for the 15 mM SDS sample. Hence the molar ratio SDS:carbetocin of 1:1 seems to be where the two types of molecules affect each other the most. The above reasoning does not correlate with the dNMR data (Figure 11) at

a first glance, which suggest that the aggregates are largest at the highest SDS concentration. However, here one needs to remember that the observed D values, are the weighted average of all possible aggregates, including monomers. Since the D is higher for monomers (almost one order of magnitude [40], the observed D (Equation 4) will be affected more by the monomers compared to the aggregates with lower D values even though there are as many surfactants residing in micelles as there are free surfactants. In the 15 mM SDS solution, a larger fraction of the surfactant molecules are monomers compared to the 100 mM SDS solution where a majority of surfactants reside in micelles. Since the diffusion coefficients for the 15 mM SDS sample and the 100 mM SDS sample are almost the same, the aggregates in the 15 mM sample must be larger than the ones in the 100 mM sample, in order for the equation to make sense.

What could have affected the surfactant-carbetocin results is that the addition of carbetocin may affect the CMC of the surfactants and hence the fraction surfactants residing in micelles at a certain concentration cannot be determined. The CMC could potentially go from 8 mM to 4 mM when carbetocin is added which would markedly alter the fraction of surfactants residing in micelles at the 15 and 45 mM SDS samples, and hence the above reasoning might be somewhat faulty.

If this interaction between SDS and carbetocin affects the soluble aggregation of carbetocin (which is the major problem of concern in this work) is hard to tell. However, one could assume that several carbetocin molecules bind in to the same micelle, since the aggregation number (how many surfactants there are in each micelle) of SDS is quite large around 60-100 [37][38] and the D values of carbetocin and SDS are almost the same in the 45 mM SDS sample (Figure 11). At this concentration, there are many more carbetocin molecules compared to micelles, hence the above assumption. If that is the case, the carbetocin molecules are closer to each other when bound to micelles than they would be free in solution, the concentration of carbetocin is locally increased. And hence, the aggregation can increase when SDS is added, however, this is not investigated in this work and further research is needed to conclude whether or not this is the case.

Since a hydrophobic interaction was believed to be important in the SDS-carbetocin interaction one could suggest that the hydrophobic parts of carbetocin reside in interior of the micelle. Since the micelle interior is hydrophobic, this would be a favorable environment for these hydrophobic carbetocin sites. However, above it was suggested that hydrophobic interaction was of importance in the self-aggregation of carbetocin, but in this new environment (carbetocin residing in a micelle) we suggest that it is other forces that are important for carbetocin self-aggregation, probably hydrogen bonding, since the hydrophobic parts of carbetocin are already interacting favorable with SDS.

For the surfactant with a larger head group ($C_{12}E_5$), changes in the appearance of the tyrosine peaks are detected as well (Figure 14) indicating that carbetocin self-aggregation occurs or that the tyrosine residue is involved in the formation of mixed aggregates. Concerning the dNMR results (Figure 13), there are results worth discussing. When a small amount of $C_{12}E_5$ (0.12 mM) is added to a 15 mM carbetocin solution the diffusion coefficient for carbetocin is reduced compared to a reference sample of 15 mM carbetocin. For 0.12 mM $C_{12}E_5$, the diffusion coefficient is increased in presence of 15 mM carbetocin compared to a reference sample. This indicates that the micelles formed at 0.12 mM surfactant concentration (CMC=0.06 mM) are larger than the micelles formed when carbetocin is present. It is known that $C_{12}E_5$ normally forms large micellar structures [43]. The addition of carbetocin

is then believed to reduce the size of these micelles by being incorporated in them. Compared to SDS, where it seems like carbetocin increases the size of the micelles, for $C_{12}E_5$ it seems to be the opposite. This difference in behavior is probably due to the difference in structure of the hydrophilic heads of SDS and $C_{12}E_5$. The reduction in D for carbetocin in the 0.12 mM $C_{12}E_5$ solution indicates that some carbetocin molecules reside in the micelles. The decrease in D values for $C_{12}E_5$ for concentrations >0.12 mM is probably due to the larger extents of surfactant molecules that reside in micelles. Worth to note here, as also explained for the SDS above, is that monomers contribute more to the observed D (D_{obs}), Equation 4, since they have much larger D values. It could be that the distinct decrease in $C_{12}E_5$ D value between 0.12 to 15 mM is partly due to this and not a major change in the actual size of the micelles. At the 45 mM $C_{12}E_5$ concentration, the diffusion coefficient for carbetocin decreases, which implies that a larger amount of the carbetocin molecules reside in micelles and for the highest $C_{12}E_5$ concentration, the D for carbetocin is the same as for $C_{12}E_5$ which implies that the majority of carbetocin molecules reside in micelles.

With the same arguments as for SDS, it is believed that the self-aggregation of carbetocin may increase in the presence of $C_{12}E_5$. Because of this local increase in carbetocin concentration there is a higher risk of carbetocin aggregates being formed. Previous studies have shown that phase-separated carbetocin aggregation increases in the presence of SDS and $C_{12}E_5$ [6].

9.3 Viscosity

Apart from the uses of viscosity data when analyzing dNMR results, they can in themselves be of interest to this project since changes in aggregation behavior often affect the viscosity as well. Results from Table 1 are discussed in this section. The viscosities of low carbetocin concentrations are not significantly larger than the viscosity of water (0.94 cm^2/s for 14 mM and 0.91 cm^2/s for 5 mM), however, at higher concentrations (47 mM) a notable increase is observed, 1.1 cm^2/s. This increase in viscosity may be due to that some kind of aggregates are forming, however, as mentioned in 8.4 the structure of these aggregates cannot be determined either from the viscosity measurements nor the NMR analysis being performed. For future studies, one could try to determine the structure by using high-resolution microscopes such as cryo-electron microscopy or some kind of light scattering technique. The viscosity results for SDS-carbetocin mixtures follow the expected trend, as explained in the NMR analysis section 9.2, with higher SDS concentration and more micelles in the solution, the viscosity increases. For $C_{12}E_5$, the results also relate to the dNMR results. The viscosity of $C_{12}E_5$ 15 mM and carbetocin 15 mM (1.01 cm^2/s) is lower than for the reference sample of only $C_{12}E_5$ 15 mM (1.33 cm^2/s). This is in line with what was discussed in section 9.2, that carbetocin disrupts the large micelles and smaller micelles are formed. That these larger micelles (often rod-like in structure), which are present with no carbetocin added, have a higher viscosity is expected[18].

10 Conclusions

Carbetocin forms some kind of aggregates in solution, in which hydrophobic interactions and hydrogen bonding are likely involved. This aggregation increases with peptide concentration. The tyrosine residue of carbetocin seems to be the major site of hydrophobic interaction and the carbonyl oxygen and amide protons of the peptide backbone the contributors to the hydrogen bonding. There appears to be a critical concentration (around 15-20 mM) above which larger aggregates are formed. Carbetocin strongly interact with SDS and $C_{12}E_5$, changing the structure of the micelles and it is believed that the self-aggregation of carbetocin is increased in the presence of these surfactants, potentially a pre-structure to phase-separated aggregates. A molar ratio of 1 in a SDS-carbetocin solution affects the ^{1}H NMR spectrum most. The viscosity of $C_{12}E_5$ changes when carbetocin is present which suggest that the structure of the $C_{12}E_5$ is altered when carbetocin reside in the micelles. NMR spectroscopy can be used to study peptide aggregation. ^{1}H NMR in itself is not sufficient to study peptide aggregation, however, combined with dNMR the results from ^{1}H NMR can be related to the aggregation. Although to better understand a system additional analytical methods should be used.

11 Future work

This work has contributed to the understanding of carbetocin aggregation. However, to fully understand the mechanisms behind the aggregation and being able to apply the knowledge to pharmaceutical applications, more research is needed. The contradictory results of this work and [6] concerning the involvement of the tyrosine residue in the interaction with SDS should for example be investigated further. Additionally, a more detailed dNMR analysis of carbetocin around 15 – 20 mM could possibly deduce if there is a CAC and if so which value is critical. Also, to obtain additional information on the structure of the soluble aggregates would be valuable. The interactions between carbetocin and the surfactants are interesting and could if investigated further contribute to the basic understanding of peptide surfactant interaction. However, for pharmaceutical applications it would be suggested that carbetocin together with approved excipients should be studied further.

12 References

[1] K. Fosgerau and T. Hoffmann, “Peptide therapeutics: Current status and future directions,” *Drug Discov. Today*, vol. 20, no. 1, pp. 122–128, 2014.

[2] P. Vlieghe, V. Lisowski, J. Martinez, and M. Khrestchatisky, “Synthetic therapeutic peptides: science and market,” *Drug Discov. Today*, vol. 15, no. 1/2, pp. 40–56, 2010.

[3] M. E. Aulton and K. M. G. Taylor, *Aulton’s Pharmaceutics: The design and manufacture of medicines*, 5th ed. Elsevier Health Sciences, 2017.

[4] C. Avanti, “Innovative strategies for stabilization of therapeutic peptides in aqueous formulations,” University of Groningen, 2012.

[5] U. B. Høgstedt, “Formulation of concentrated peptide solutions - physical stability challenges and the impact of peptide-peptide interactions,” University of Copenhagen, 2017.

[6] U. B. Høgstedt, J. Östergaard, T. Weiss, H. Sjögren, and M. van der Weert, “Manipulating the aggregation behavior of the uncharged peptide carbetocin,” *J. Pharm. Sci.*, vol. 107, no. 3, pp. 838–747, 2017.

[7] M. Widmer, G. Piaggio, H. Abdel-Aleem, G. Carroli, Y.-S. Chong, A. Coomarasamy, B. Fawole, S. Goudar, G. J. Hofmeyr, P. Lumbiganon, K. Mugerwa, T. M. H. Nguyen, Z. Quershi, J. P. Souza, and A. M. Gülmezoglu, “Room temperature stable carbetocin for the prevention of postpartum haemorrhage during third stage labour in women delivering vaginally: study protocol for a randomized controlled trial,” *Trials*, vol. 17, no. 143, 2016.

[8] X. Meng, F. Shen, C. Li, Y. Li, and X. Wang, “Depression-like behaviors in tree shrews and comparison of the effects of treatment with fluoxetine and carbetocin,” *Pharmacol. Biochem. Behav.*, vol. 145, pp. 1-8, 2016.

[9] Y. Cohen, L. Avram, and L. Frish, “Diffusion NMR spectroscopy in supramolecular and combinatorial chemistry: An old parameter - New insights,” *Angew. Chemie - Int. Ed.*, vol. 44, no. 4, pp. 520–554, 2005.

[10] M. Alajarín, A. Pastor, R.-A. Orenes, E. Martínez-Viviente, and P. S. Pregosin, “Pulsed gradient spin echo (PGSE) diffusion measurements as a tool for eludication of a new type of hydrogen-bonded bicapsular aggregate,” *Chem. - A Eur. J.*, vol. 12, no. 3, pp. 877–886, 2006.

[11] K. Teilum, B. Halle, S. Linse, K. Modig, and I. Andre, *Biophysical Chemistry*. Media-Tryck, Lund University, 2017.

[12] M. C. Manning, D. K. Chou, B. M. Murphy, R. W. Payne, and D. S. Katayama, “Stability of protein pharmaceuticals: An update,” *Pharmaceutical Research*. 2010.

[13] D. Horinek, M. Serr, M. Geisler, T. Pirzer, U. Slotta, S. Q. Lud, G. J.A., T. Scheibel, T. Hugel, and R. R. Netz, “Peptide adsorption on a hydrophobic surface results from an interplay of solvation, surface, and intrapeptide forces,” *Proc. Natl. Acad. Sci.*, vol. 105, no. 8, pp. 2842–2847, 2008.

[14] Y. Wei and A. L. Robert, “Benchmark experimental data set and assessment of adsorption free energy for peptide-surface interactions,” *Langmuir*, vol. 25, no. 10, pp. 5637–5646, 2009.

[15] C. J. Roberts, “Therapeutic protein aggregation: mechanisms, design, and control,” *Trends Biotechnol.*, vol. 32, no. 7, pp. 372–380, 2014.

[16] R. W. Payne and M. C. Manning, "Peptide Formulation: Challenges and Strategies," *Innov. Pharm. Technol.*, vol. 28, no. 64–68, 2009.

[17] S. J. Shire, Z. Shahrokh, and J. Liu, "MINIREVIEW Challenges in the Development of High Protein Concentration Formulations," *Pharm. Assoc. J Pharm Sci*, vol. 93, pp. 1390–1402, 2004.

[18] B. Kronberg, K. Holmberg, and B. Lindman, *Surface chemistry of surfactants and polymers*. John Wiley & Sons, 2014.

[19] C. M. Dobson, "Protein folding and unfolding," *Nature*, vol. 426, no. 6968, p. 884, 2003.

[20] C. M. Dobson, "Getting out of shape," *Nature*, vol. 418, no. 6899, 2002.

[21] L. S. Meshykhi, M. R. Nel, and D. N. Lucas, "The role of carbetocin in the prevention and management of postpartum haemorrhage,"*Obstetric anesthesia digest*, vol. 37, no. 3, pp. 115-116, 2017.

[22] J. Shaji and V. Patole, "Protein and peptide drug delivery: oral approaches," *Indian J. Pharm. Sci.*, vol. 70, no. 3, pp. 269–277, 2008.

[23] T. J. Kamerzell, R. Esfandiary, S. B. Joshi, C. R. Middaugh, and D. B. Volkin, "Protein-excipient interactions: Mechanisms and biophysical characterization applied to protein formulation development," *Adv. Drug Deliv. Rev.*, vol. 63, no. 13, pp. 1118–1159, 2011.

[24] W. Wang, S. Nema, and D. Teagarden, "Protein Aggregation - pathways and influencing factors," *Int. J. Pharm.*, vol. 390, pp. 89–99, 2010.

[25] A. P. Sherje, B. R. Dravyakar, D. Kadam, and M. Jadhav, "Cyclodextrin-based nanosponges : A critical review," vol. 173, no. 1, 2017.

[26] A. Harada, Y. Takashima, and H. Yamaguchi, "Cyclodextrin-based supramolecular polymers," *Chem. Soc. Rev.*, vol. 38, no. 4, p. 875, 2009.

[27] T. Irie, "Cyclodextrins in peptide and protein delivery," *Adv. Drug Deliv. Rev.*, vol. 36, no. 1, pp. 101–123, 1999.

[28] M. V. Rekharsky and Y. Inoue, "Complexation Thermodynamics of Cyclodextrins," *Chem. Rev.*, vol. 98, no. 5, pp. 1875–1918, 1998.

[29] T. D. W. Claridge, *High-Resolution NMR Techniues in Organic Chemistry*. Elsevier Science, 1999.

[30] J. Keeler, *Understandning NMR Spectroscopy*, 1st ed. John Wiley & Sons, 2005.

[31] C. F. Tormena, "Conformational analysis of small molecules: NMR and quantum mechanics calculations," *Prog. NMR Spectrosc.*, vol. 96, pp. 73–88, 2016.

[32] P. Stilbs, "Fourier Pulsed-Gradient Studies of Molecular Diffusion," *Prog. NMR Spectrosc.*, vol. 19, pp. 1–45, 1987.

[33] E. L. Hahn, "Spin echoes," *Phys. Rev.*, vol. 80, no. 4, 1950.

[34] E. O. Stejskal and J. E. Tanner, "Spin diffusion measurements: spin echoes in the presence of a time-dependent field gradient," *J. Chem. Phys.*, vol. 42, no. 1, pp. 288–292, 1965.

[35] P. Stilbs, "Fourier transform pulsed-gradient spin-echo studies of molecular diffusion," *Prog. Nucl. Magn. Reson. Spectrosc.*, vol. 19, no. 1, pp. 1–45, Jan. 1987.

[36] J. Des Cloizeaux and Ge. Jannink, *Polymers in solution: their modelling and structure*. OUP Oxford, 2010.

[37] P. Cioni and G. B. Strambini, “Effect of heavy water on protein flexibility,” *Biophys. J.*, vol. 82, no. 6, pp. 3246–3253, 2002.

[38] L. Korson, W. Drost-Hansen, and F. J. Millero, “Viscosity of water at various temperatures,” *J. Phys. Chem.*, vol. 73, no. 1, pp. 34–39, 1969.

[39] D. Lundberg, J. Unga, A. L. Galloway, and F. M. Menger, “Studies on ester-modified cationic amphiphile in aqueous systems: Bahvior of binary solutions and ternary mixtures with conventional surfactants,” *Langmuir*, vol. 23, no. 23, pp. 11434–11442, 2007.

[40] D. G. Leaist, “Binary diffusion of micellar electrolytes,” *J. Colloid Interface Sci.*, vol. 111, no. 1, pp. 230–239, 1986.

[41] M. Almgren and S. Swarup, “Size of sodium dodecyl sulfate micelles in the presence of additives i. alcohols and other polar compounds,” *J. Colloid Interface Sci.*, vol. 91, no. 1, pp. 256–266, 1983.

[42] N. A. Mazer, G. B. Benedek, and M. C. Carey, “An investigation oof the micellar phase of sodium dodecyl sulfate in aqueous sodium chloride solutions using quasielastic light scattering spectroscopy,” *J. Phys. Chem.*, vol. 80, no. 10, pp. 1075–1085, 976.

[43] M. Jonstroemer, B. Joensson, and B. Lindman, “Self-diffusion in nonionic surfactant-water systems,” *J. Phys. Chem.*, vol. 95, no. 7, pp. 3293–3300, 1991.

13 Appendices

13.1 Populärvetenskaplig sammanfattning

NMR-studie av aggregringen hos den terapeutiska peptiden carbetocin

Visst vore det bra om färre kvinnor dör som följd av komplikationer vid förlossning, eller att ett nytt läkemedel mot depression kommer ut på marknaden? Med mer insikt om ett biologiskt läkemedels fysikaliska stabilitet kan detta bli verklighet. I detta mastersarbete har det biologiska läkemedlet carbetocin studerats med avseende på just detta.

Vanliga läkemedel som vi är vana vid att ta i tablettform består oftast av små molekyler. Det finns dock vissa sjukdomar och tillstånd som inte kan behandlas med dessa små oftast kemiskt framställda molekyler, då finns det (kanske) biologiska läkemedel att tillgå. Biologiska läkemedel är läkemedel av biologisk härkomst, ett exempel på detta är peptidbaserade läkemedel. En peptid är biologisk molekyl som består av aminosyror, en kemisk enhet som bygger upp alla proteiner. En peptid består av färre aminosyror och saknar den 3D-struktur som proteiner har, men i grunden är de lika. Carbetocin är en peptid som används för att behandla onormal mängd blödning efter förlossning. Carbetocin är en modifierad variant av hormonet oxytocin vilket bland annat ”orsakar” sammandragningar av livmodern vid förlossning. Carbetocin är den peptid som har studerats i detta projekt.

På grund av att carbetocin och andra peptider har ett biologiskt ursprung fungerar de på ett annorlunda sätt än traditionella läkemedel. Ett problem är hantering och förvaring, att de måste hålla sig stabila innan de ges till en patient. Med stabilitet menas här att läkemedlet behåller sin terapeutiska effekt och inte blir skadlig för patienten. Ett stabilitetsproblem som ofta dyker upp för peptider (och proteiner) är aggregering. Aggregering är när partiklar (eller molekyler i det här fallet) interagerar och bildar en större partikel (eller ett aggregat av molekyler). Fokusen för detta arbete var att studera och försöka förstå hur carbetocin aggregerar.

För att studera detta fenomen, användes NMR spektroskopi vilket är en teknik som bygger på samma grundprinciper som en MR-kamera. Med denna teknik kan egenskaper kring enstaka atomer i en molekyl analyseras. Genom att studera carbetocin tillsammans med olika tillsatser, fick vi fram att aggregeringen är väldigt koncentrations- och temperaturberoende och vilka delar i peptiden som spelar en stor roll i aggregeringen och därav vilka mekanismer som sannolikt ligger bakom aggregeringen. Det kan vara så att det krävs en viss minimi-koncentration av carbetocin för att aggregering ska uppstå, under vilken aggregeringen är knappt märkbar och att så kallade tensider har en stor påverkan på aggregeringsbeteendet.

Med detta bidrag till en djupare förståelse av carbetocins stabilitet, kan förhoppningsvis läkemedel med nya tillsatser forskas fram som gör läkemedlet bättre och mer tillgängligt för kvinnor som behöver det. Denna förståelse kan i förlängningen också leda till nya läkemedelstillsatser som gör det möjligt att ha en högre peptidkoncentration. En applikation av detta är att använda carbetocin som ett depressionsdämpande läkemedel vilket det enligt forskning finns en möjlighet till men att det då krävs en högre koncentration av peptiden jämfört med när man behandlar förlossningsproblem. Generellt, ger en djupare förståelse för läkemedlets aktiva ingrediens (peptiden i detta fall) större möjligheter att utveckla ett bättre och mer effektivt läkemedel.

13.2 Temperature dependence

The spectra of higher temperatures in Figure 17 and Figure 18 were more similar in appearance and chemical shifts, to a spectrum of higher carbetocin concentration at 25 °C, indicating that aggregation is increased at a higher temperature, since it is known that aggregation increases at higher concentrations.

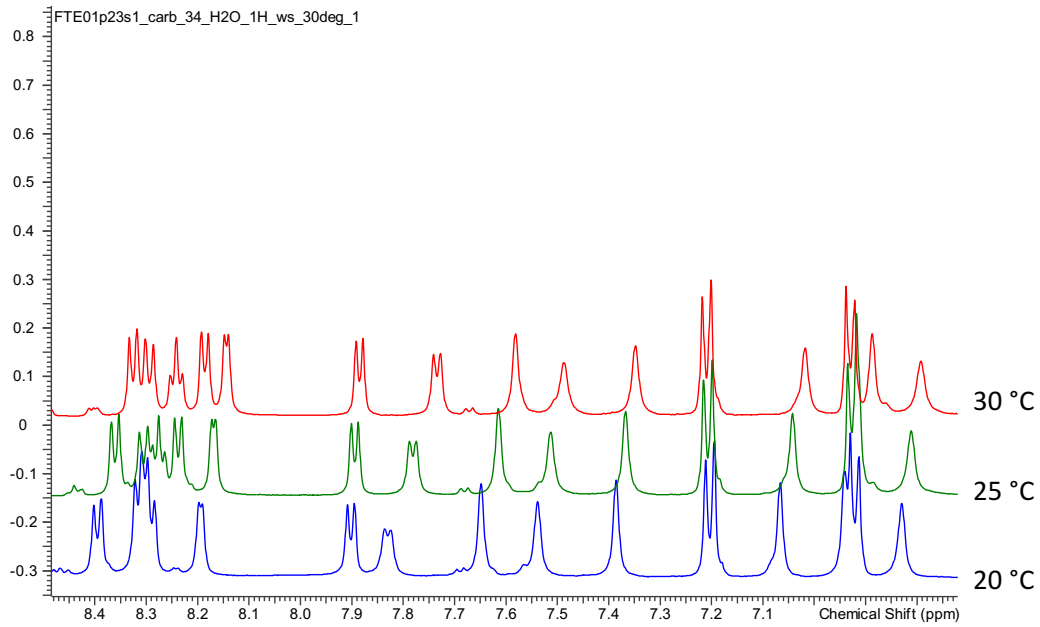

Figure 17: ^{1}H NMR spectra of 34 mM carbetocin at three different temperatures. From the top, red: 30°C, green: 25°C and blue: 20°C.

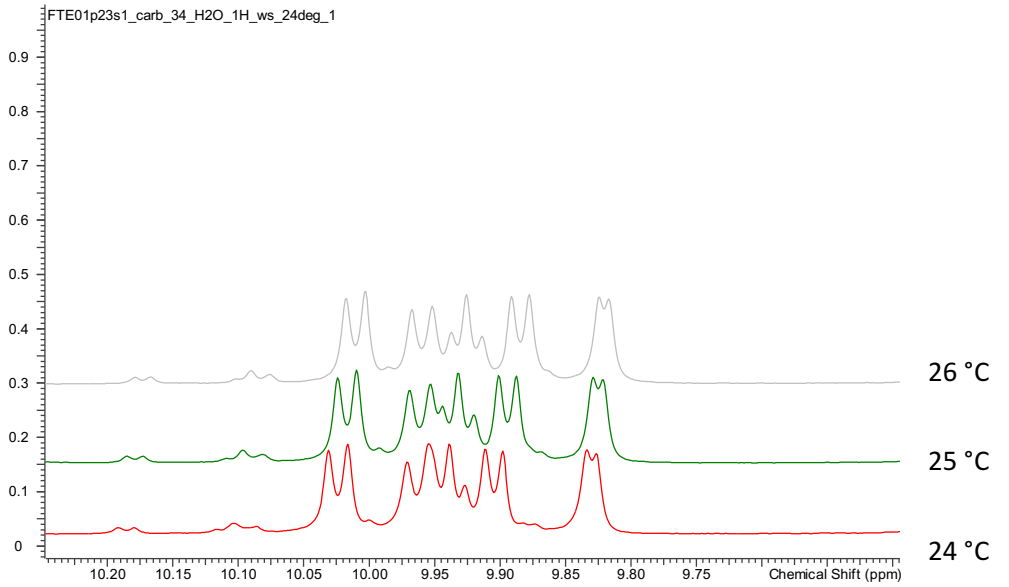

Figure 18: ^{1}H NMR spectrum of 34 mM carbetocin at three different temperatures. From the top, grey: 26°C, green: 25°C and red: 24°C.

13.3 Temperature Calibration

A spectrometer often shows a value for temperature; however, this needs calibration. By taking a spectrum of a substance with a well-known temperature dependence, the temperature can be calibrated. The standard is to use methanol for temperatures ranging 175-310 K, which is the range all experiments in the project is performed in, and ethylene glycol for 300-400 K. The methanol NMR spectrum has two distinct peaks and by measuring the difference in chemical shifts, Equation 6 is used to get the temperature [29].

$$T = 403 - 29.53\Delta\delta - 23.87(\Delta\delta)^2 \qquad \text{Equation 6}$$

For ethylene glycol, there is another equation, Equation 7.

$$T = 466 - 101.6\Delta\delta \qquad \text{Equation 7}$$

13.4 NMR Assignment

Figure 19 and Figure 20 explain how the protons and carbons are named in the assignment tables below,

Table 3 and Table 4.

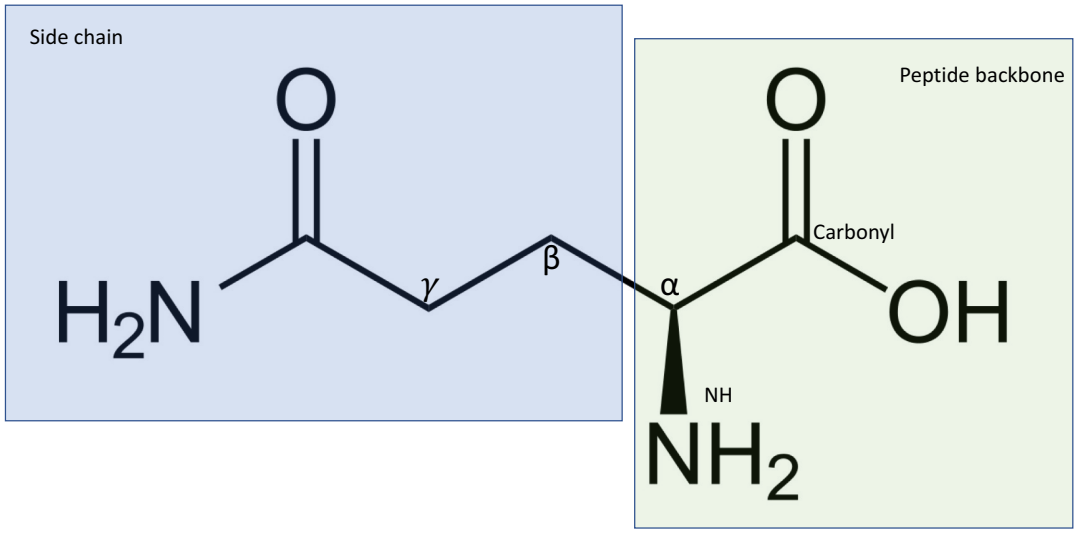

Figure 19: Amino acid structure with naming of the different positions (Carbonyl, NH, α, β, and γ).

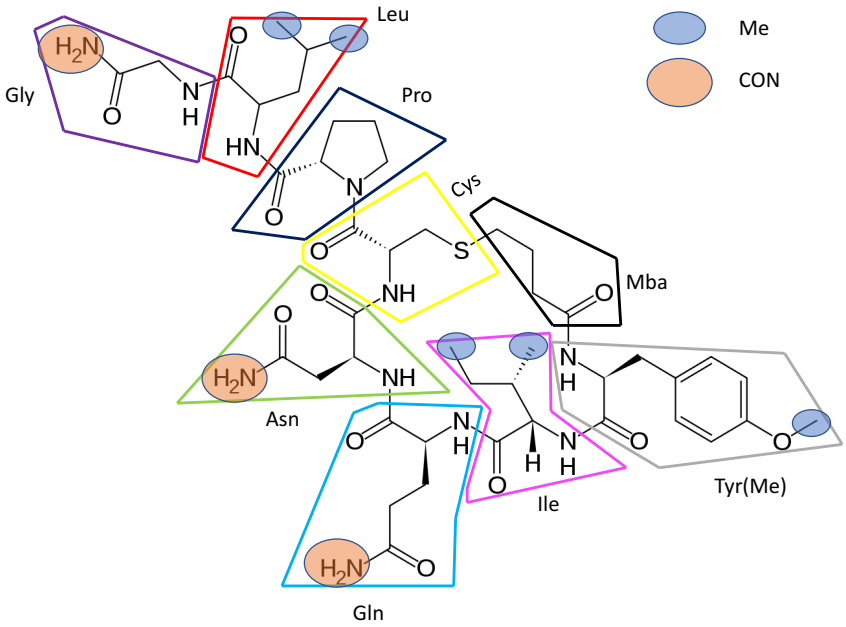

Figure 20: Molecular structure of carbetocin with amino acid residues marked and their abbreviations. Certain entities are also pointed out with their abbreviations (Me and CON).

Below (Figure 21-Figure 25) are the ^{1}H, ^{13}C, COSY, ROESY and HSQC spectra used during the assignment process. Data provided by Ferring (not published) was also used for the assignment.

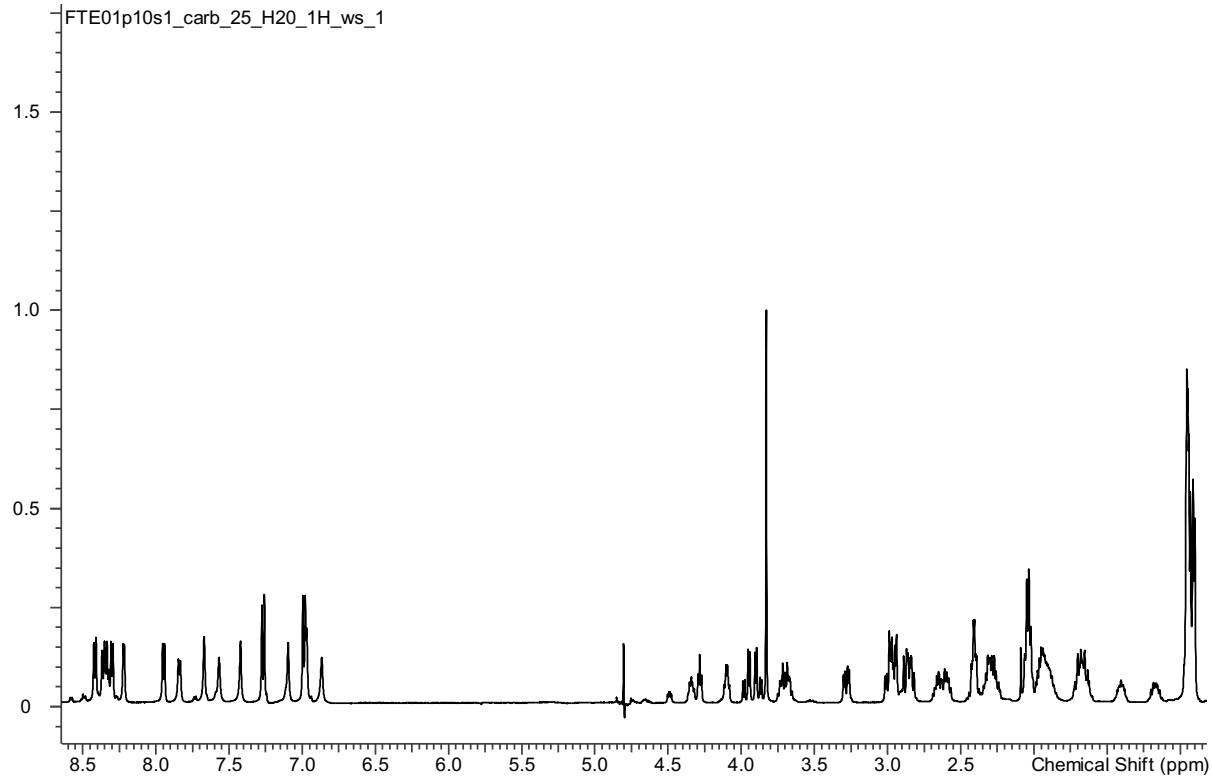

Figure 21: ^{1}H NMR spectrum of 25 mM carbetocin in water.

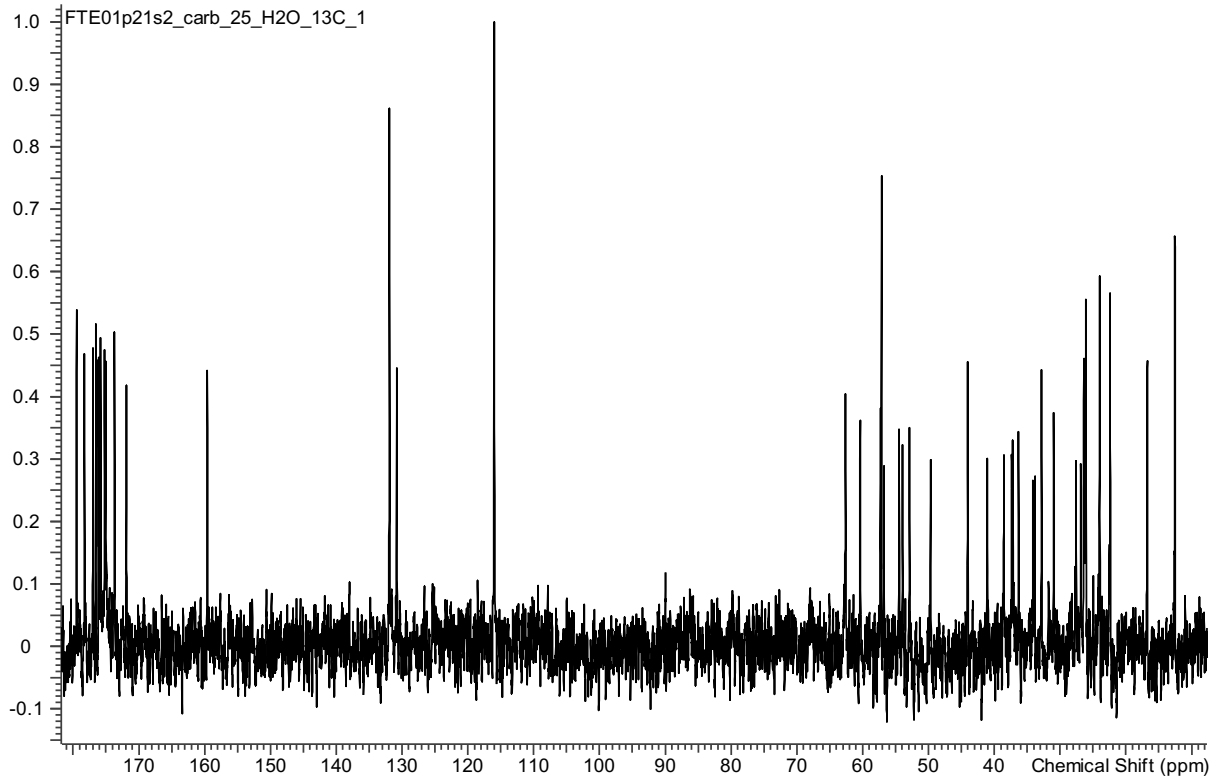

Figure 22: ^{13}C NMR spectrum of 25 mM carbetocin in water

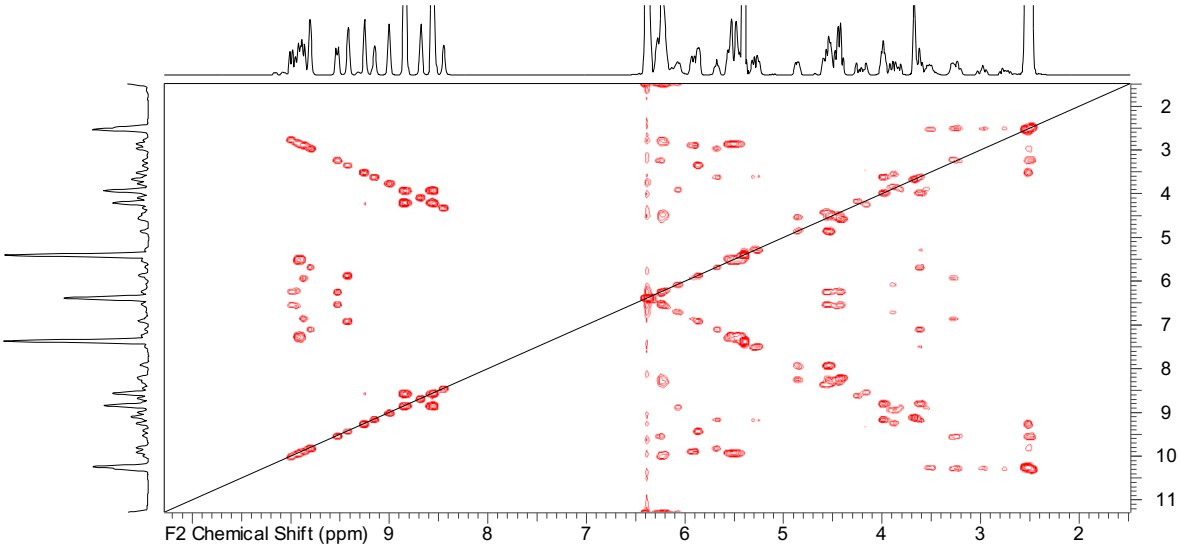

Figure 23: $^{1}H^{1}H$ COSY spectrum of 32 mM carbetocin.

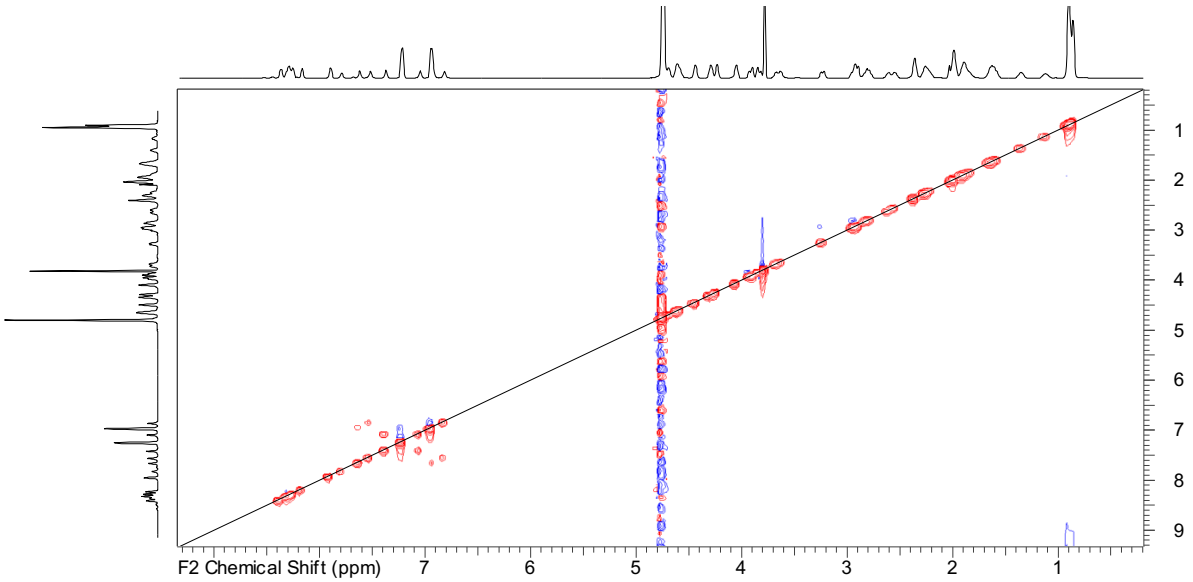

Figure 24: ROESY spectrum of 15 mM carbetocin.

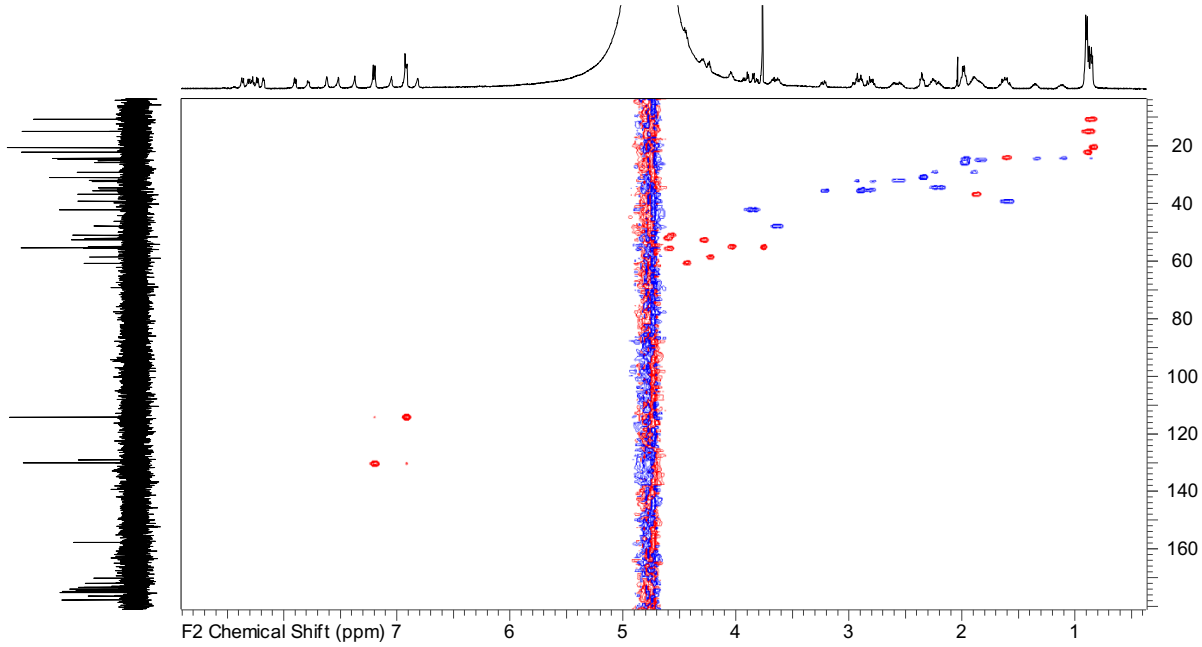

Figure 25:HSQC spectrum of 47 mM carbetocin

Table 3 and Table 4 show the assignment for the proton respectively carbon spectra.

Table 3: Proton Assignment

Proton	^{1}H Chemical shift (ppm)
MeγLeu	0.9-0.95
MeβIle	0.9-0.95
MeγIle	0.9-0.95
MeγLeu	0.9-0.95
γHile	1.17
γHile	1.40
βH2Leu	1.65-1.70
γHleu	1.65-1.70
βHIle	1.94-1.96
γHMba?	1.94-2.03
βH2Mba?	1.94-2.03
γH2Pro?	1.94-2.03
bH2Gln	2.03
γHmba?	2.25-2.35
bH2Pro?	2.25-2.35
γH2Gln	2.40
αH2mba?	2.55
βH2Tyr(me)	2.80-3.00
βH2Asn	2.80-3.00
βHCys	2.80-3.00
βHCys	3.25
δH2Pro	3.69

MeTyr(Me)	3.83
αH2Gly	3.85-3.99
αHGln	4.09
αHIle	4.27
αHLeu	4.29
αHPro	4.49*
αHAsn	4.49-4.51*
αHTyr(Me)	4.49-4.51*
αHCys	4.49-4.51*
CONHGln or CONHAsn	6.87
mC6H4Tyr(Me)	6.98-6.99
CONHGly	6.98-6.99
CONHAsn or CONHGln	7.10
oC6H4Tyr(Me)	7.26
CONHAsn or CONHGln	7.42
CONHGln or CONHAsn	7.51
CONHGly	7.67
NHIle	7.80
NHGln	8.30
NHLeu	8.33
NHGly	8.35
NHCys?	8.4-8.45. or 8.0
NHTyr(Me)?	8.4-8.45. or 8.0
NHAsn?	8.4-8.45. or 8.0

* Not visible in provided spectrum

Table 4: Carbon assignment

Carbon	^{13}C chemical shift ppm
MeγIle	10.70
MeβIle	16.74
MeγLeu	22.38
MeγLeu	23.98
γLeu	26.07
γIle	26.20
γPro	26.37
βMba?	26.80
βGln	27.56
γMba?	31.80
γGln	32.80
βPro?	33.80
βAsn	34.05
αMba?	36.30
βTyr(Me)?	37.18
βCys	37.34
βIle	41.10
βLeu	44.02
αGly(NH2)	49.50
δPro	49.84
αAsn?	52.88. 53.93 or 57.13
αCys?	52.88. 53.93 or 57.13
αLeu	54.44
αGln	56.40

MeTyr(Me)?	52.88. 53.93 or 57.13
αTyr(Me)	57.28
αIle	60.04
αPro	62.60
mTyr(Me)	115.99
γTyr(Me)	130.81
oTyr(Me)	131.92
pTyr(Me)	159.58
Carbonyl Gly	171.89-179.46
Carbonyl Leu	171.89-179.46
Carbonyl Pro	171.89-179.46
Carbonyl Cys	171.89-179.46
Carbonyl Mba	171.89-179.46
Carbonyl Tyr(Me)	171.89-179.46
Carbonyl Ile	171.89-179.46
Carbonyl Gln	171.89-179.46
Carbonyl Asn	171.89-179.46
Carbonyl Gln side chain	171.89-179.46
Carbonyl Asn side chain	171.89-179.46

13.5 Change in chemical shifts relative to 5 mM for ^{1}H & ^{13}C NMR

Table 5: Change in chemical shift for the 50 mM sample relative to the 5 mM sample with two different reference signals from ^{1}H NMR spectra. The 7 peaks with the highest $\Delta\delta$ for both references are marked in yellow.

	Change in chemical shift between the 50 mM and 5 mM samples	
Proton name	Methyl reference	Glnβ reference
αH2Gly	0.0048	0.001
αH2Mba	0.0001	0.002
αHGln	0.003	0.0069
αHIle	0.0107	0.0068
αHLeu	0.0058	0.0029
αHPro	0.0057	0.0058
βH2Gln	0.0095	0
βH2Leu	0	0.0039
βH2Mba or γHMba or γHPro	0.0039	0.0088
βH2Tyr(Me) or βH2Asn	0.0088	0.0127
βH2Tyr(Me) or βH2Asn	0.0137	0.0078
βHCys	0.003	0.0059
βHIle	0.0029	0.0029
γH2Gln	0	0.0049
γH2Mba or bh2Pro	0.0029	0.0264
γHile	0.0049	0.0059
γHile	0.002	0.0019
γHleu	0	0
δH2Pro	0.0019	0.001
CONHAsn or CONHTyr (2)	0.0068	0.0049
CONHAsn or CONHTyr (2)	0.0049	0.001
CONHGln or CONAsn (1)	0.0029	0.0078

CONHGln or CONAsn (1)	0.002	0.0059
CONHGly	0	0.0088
CONHGly	0	0.0088
mC6H4Tyr(Me)	0.0205	0.0284
MeTyr(Me)	0.0127	0.0176
MeγLeu	0	0.002
NHCys or NHAsn or NHTyr	0.0117	0.0107
NHCys or NHAsn or NHTyr	0.0059	0.0039
NHCys or NHAsn or NHTyr	0	0.0019
NHGln	0.0234	0.0127
NHGly	0.0095	0.0206
NHIle	0.0098	0.0195
NHLeu	0.0235	0.0352
oC6H4Tyr(Me)	0.0156	0.0245

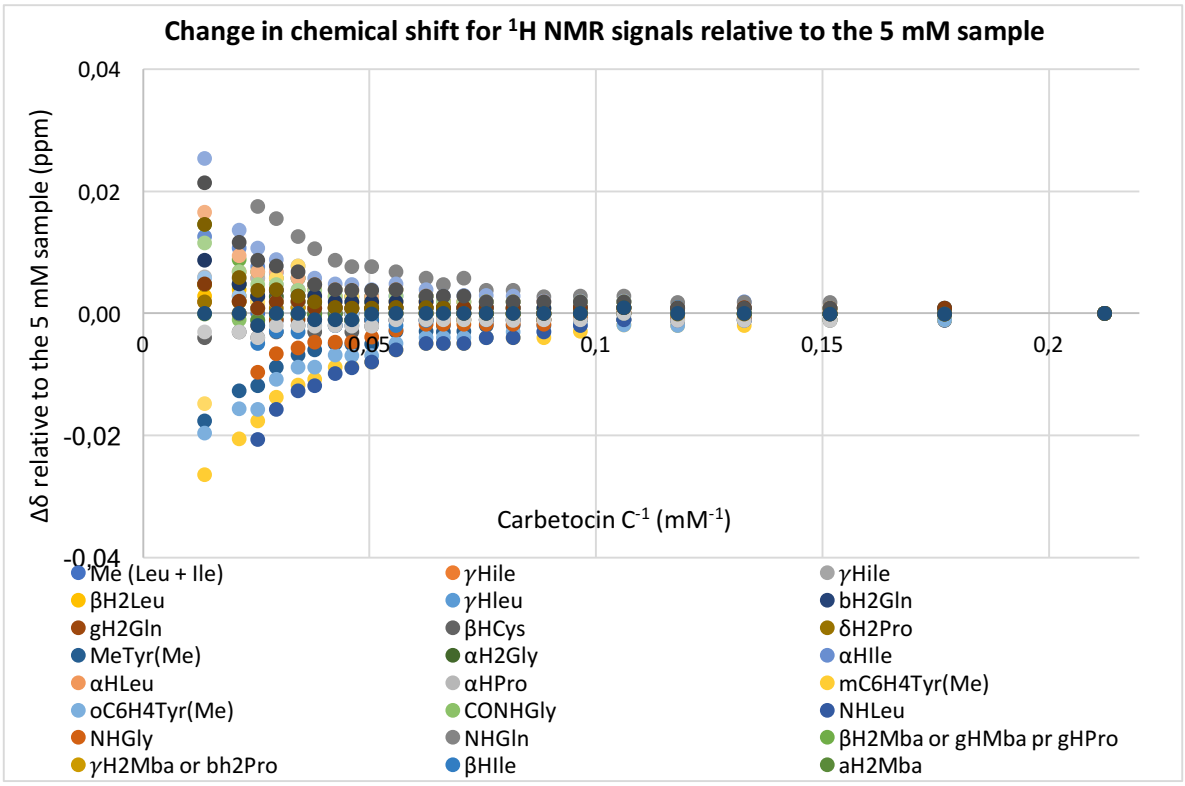

Figure 26: Chemical shifts of carbetocin in different concentrations relative to the 5 mM sample from the ^{1}H NMR data.

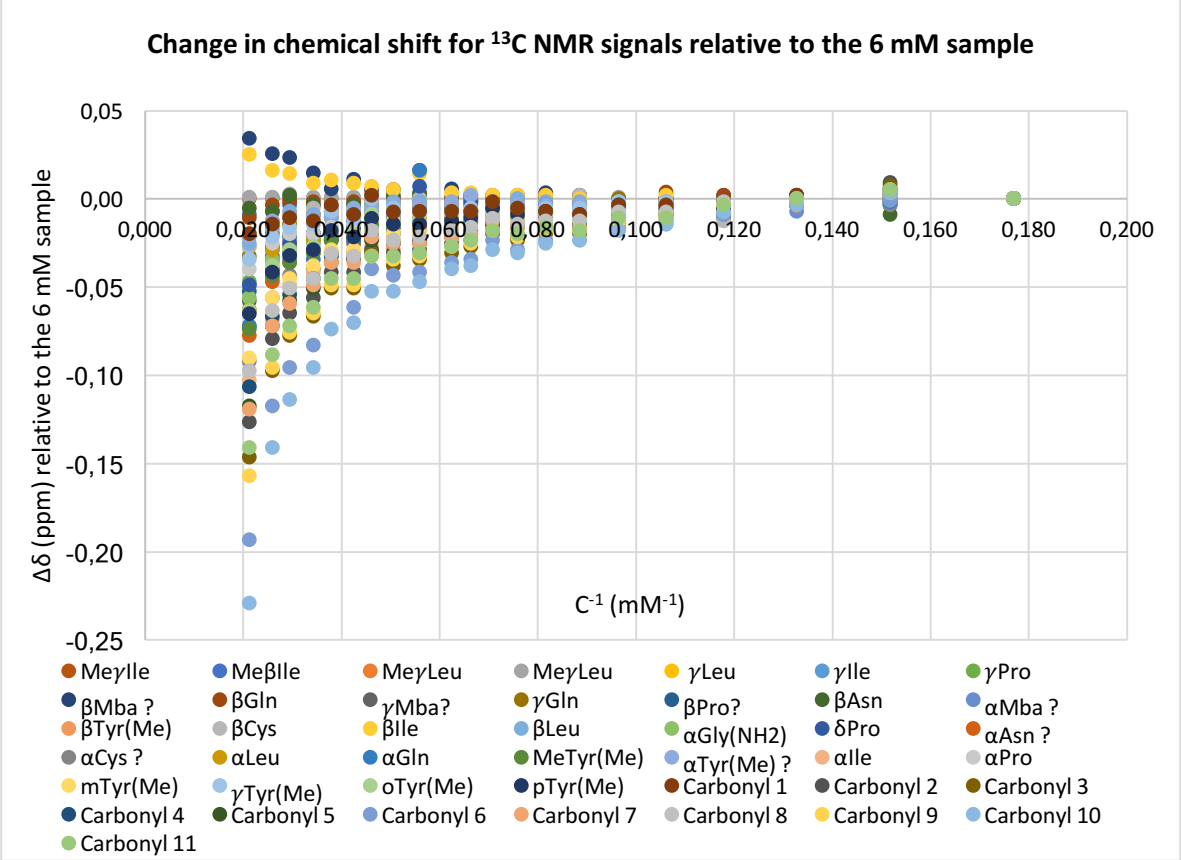

Figure 27: All chemical shifts of carbetocin in different concentrations relative to the 6 mM sample from the ^{13}C NMR data. Relative to the 6 mM sample because the 5 mM sample had a lower signal to noise ratio.

13.6 MBCD results

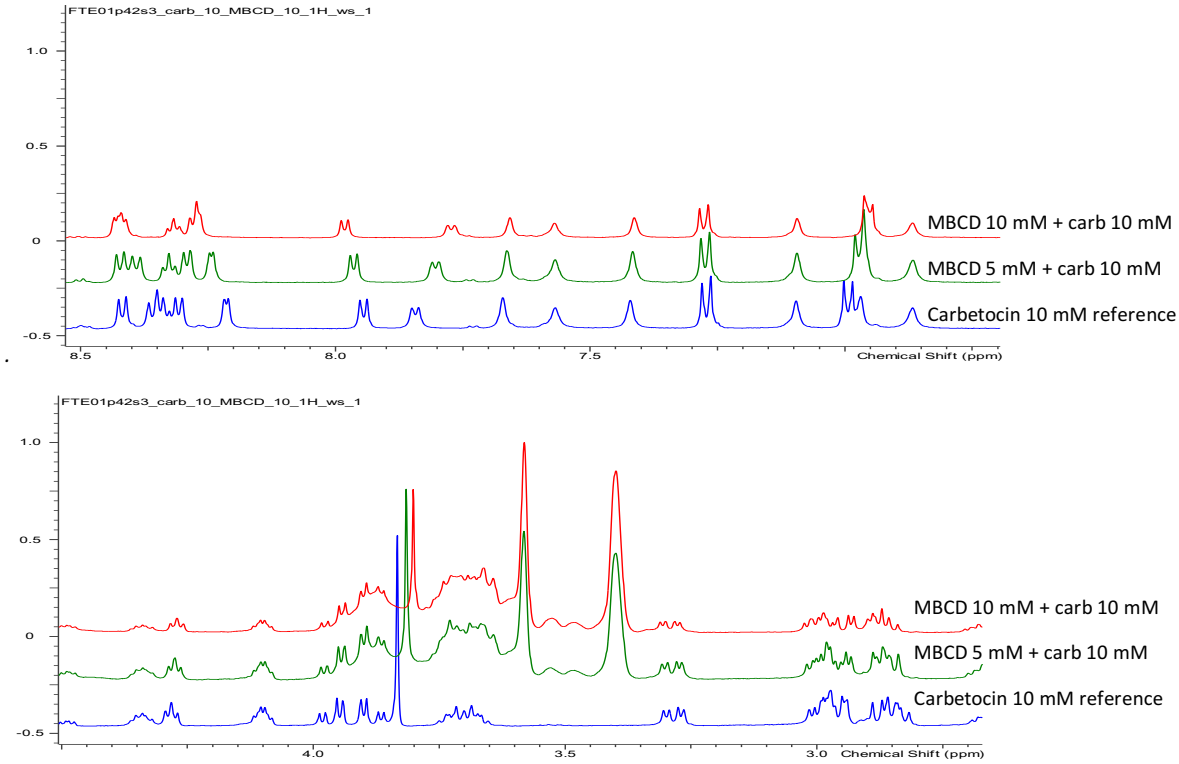

Figure 28: Parts of the spectra of MBCD-carbetocin solutions. In all samples, there are 10 mM carbetocin, Red: MBCD 10 mM, green: MBCD 5 mM and blue: only carbetocin. Note the changes around 8.3 ppm and how the peak at 3.8 ppm shifts to downfield with decreasing MBCD concentration.

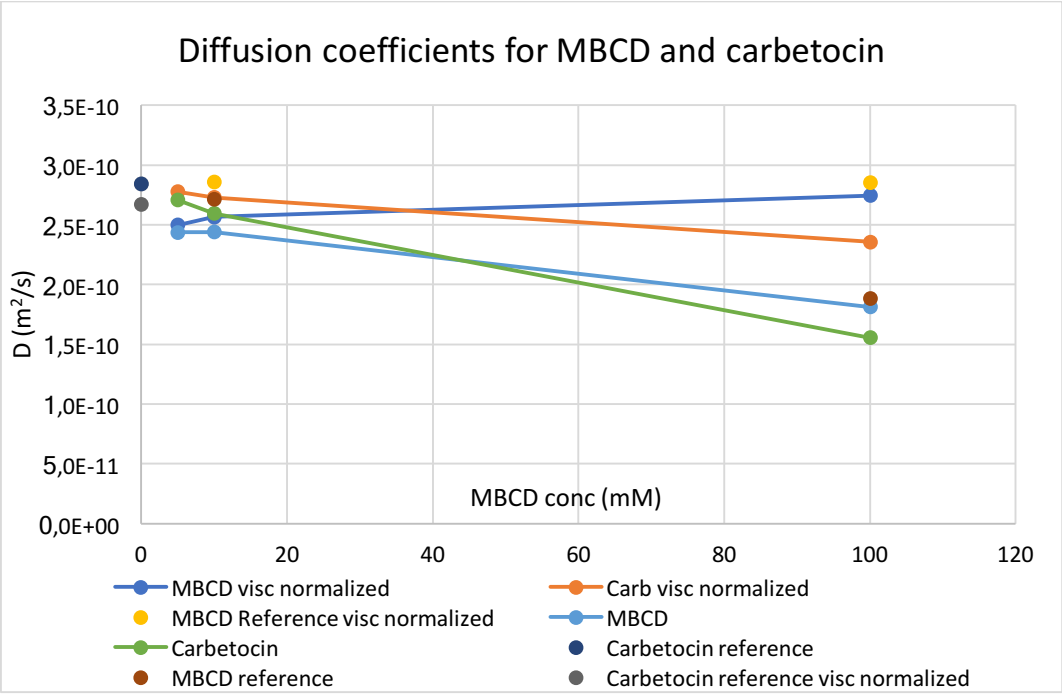

Figure 29: Diffusion coefficients of MBCD and Carbetocin of MBCD-Carbetocin solutions. Carbetocin concentration constant at 10 mM and MBCD in an increasing concentration from 5 to 100 mM.